JOURNAL OF GEOPHYSICAL RESEARCH, VOL. 111, C09039, doi:10.1029/2005JC003338, 2006

Somali Current rings in the eastern Gulf of Aden

David M. Fratantoni,[1] Amy S. Bower,[1] William E. Johns,[2] and Hartmut Peters[2]

Received 3 October 2005; revised 21 April 2006; accepted 26 May 2006; published 30 September 2006.

[1] New satellite-based observations reveal that westward translating anticyclonic rings are generated as a portion of the Somali Current accelerates northward through the Socotra Passage near the mouth of the Gulf of Aden. Rings thus formed exhibit azimuthal geostrophic velocities exceeding 50 cm/s, are comparable in overall diameter to the width of the Gulf of Aden (250 km), and translate westward into the gulf at 5–8 cm/s. Ring generation is most notable in satellite ocean color imagery in November immediately following the transition between southwest (boreal summer) and northeast (winter) monsoon regimes. The observed rings contain anomalous fluid within their core which reflects their origin in the equator-crossing Somali Current system. Estimates of Socotra Passage flow variability derived from satellite altimetry provide evidence for a similar ring generation process in May following the winter-to-summer monsoon transition. Cyclonic recirculation eddies are observed to spin up on the eastern flank of newly formed rings with the resulting vortex pair translating westward together. Recent shipboard and Lagrangian observations indicate that vortices of both sign have substantial vertical extent and may dominate the lateral circulation at all depths in the eastern Gulf of Aden.

Citation: Fratantoni, D. M., A. S. Bower, W. E. Johns, and H. Peters (2006), Somali Current rings in the eastern Gulf of Aden, *J. Geophys. Res.*, *111*, C09039, doi:10.1029/2005JC003338.

1. Introduction

[2] The Somali Current is unique among major western boundary currents in its propensity to reverse direction in response to semiannual monsoonal wind forcing [e.g., *Defant*, 1961; *Molinari et al.*, 1990]. As a consequence, the western tropical Indian Ocean is rife with eddy variability (Figure 1) over a range of temporal and spatial scales [e.g., *Schott and Quadfasel*, 1982; *Schott*, 1983; *Visbeck and Schott*, 1992]. Navigators have long been aware of several large, semipermanent recirculations near the Somali Peninsula [e.g., *Findlay*, 1866] and these eddies or gyres have been documented by numerous regional field expeditions [e.g., *Swallow and Bruce*, 1966; *Düing*, 1970; *Düing et al.*, 1980; *Bruce and Beatty*, 1985; *Fischer et al.*, 1996; *Schott and Fischer*, 2000]. The most prominent of these circulation features during the southwest (boreal summer) monsoon are the Great Whirl and the Socotra Gyre, located to the south and southeast of the island of Socotra, respectively (Figure 1). Both in situ and remote observations indicate that these features evolve slowly in time in response to the development and relaxation of the monsoon (Figure 2) but are, in general, geographically fixed [e.g., *Bruce*, 1979; *Bruce and Beatty*, 1985; *Prasad and Ikeda*, 2001; *Brandt et al.*, 2003; *Prasad et al.*, 2005].

[3] In this article we present new observations indicating that a portion of the Somali Current accelerates northward through the Socotra Passage and, constrained by the Arabian Peninsula, retroflects sharply and collapses upon itself to form discrete anticyclonic current rings which translate westward into the Gulf of Aden (GOA). In contrast to the geographically fixed features referred to above, the rings and eddies discussed herein generally result from a discrete and identifiable formation event, exhibit a measurable and sustained translation rate, and following formation, evolve independently of the regional-scale monsoon wind forcing.

[4] The present study is motivated by analysis of in situ hydrographic and direct velocity measurements collected during an investigation of the saline Red Sea outflow plume, a significant intermediate depth hydrographic feature whose signature is discernable throughout the western Indian Ocean and as far south as South Africa [*Beal et al.*, 2000]. Measurements obtained on two regional survey cruises in February–March and August of 2001 revealed that the GOA was populated by several large-diameter and vertically extensive vortices [see *Bower et al.*, 2002]. Although the ship-based observational program was ambitious (including 450 hydrographic profiles within the GOA alone), the experiment was specifically designed to sample the circulation and stratification associated with the Red Sea outflow at the extrema of monsoonal wind forcing rather than on timescales and space scales appropriate to translating mesoscale eddies. In this study we therefore rely heavily on satellite-derived remote sensing products to develop a continuous, multiyear, eddy-resolving view of the circulation in the eastern GOA.

[5] The remainder of this article is organized as follows. In section 2 we summarize the data sources and analysis

[1]Department of Physical Oceanography, Woods Hole Oceanographic Institution, Woods Hole, Massachusetts, USA.
[2]Division of Meteorology and Physical Oceanography, Rosenstiel School of Marine and Atmospheric Science, University of Miami, Miami, Florida, USA.

0148-0227/06/2005JC003338$09.00

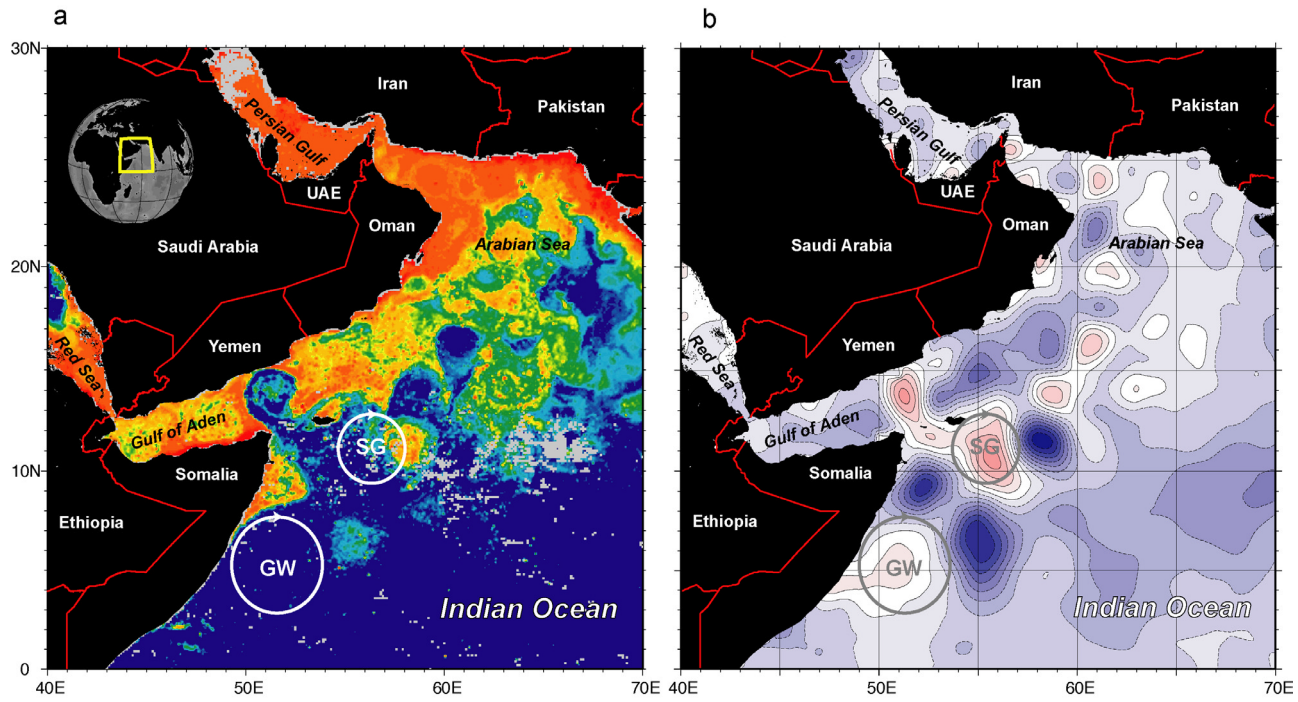

Figure 1. (a) SeaWiFS chlorophyll-a composite image (7–15 November 1999); (b) Sea level anomaly (10 November 1999) illustrating the wide range of mesoscale variability evident in the Arabian Sea and the western tropical Indian Ocean. Approximate positions of the anticyclonic Great Whirl (GW) and Socotra Gyre (SG) are schematically indicated. These images correspond to a time period immediately following the onset of the northeastern (boreal winter) monsoon.

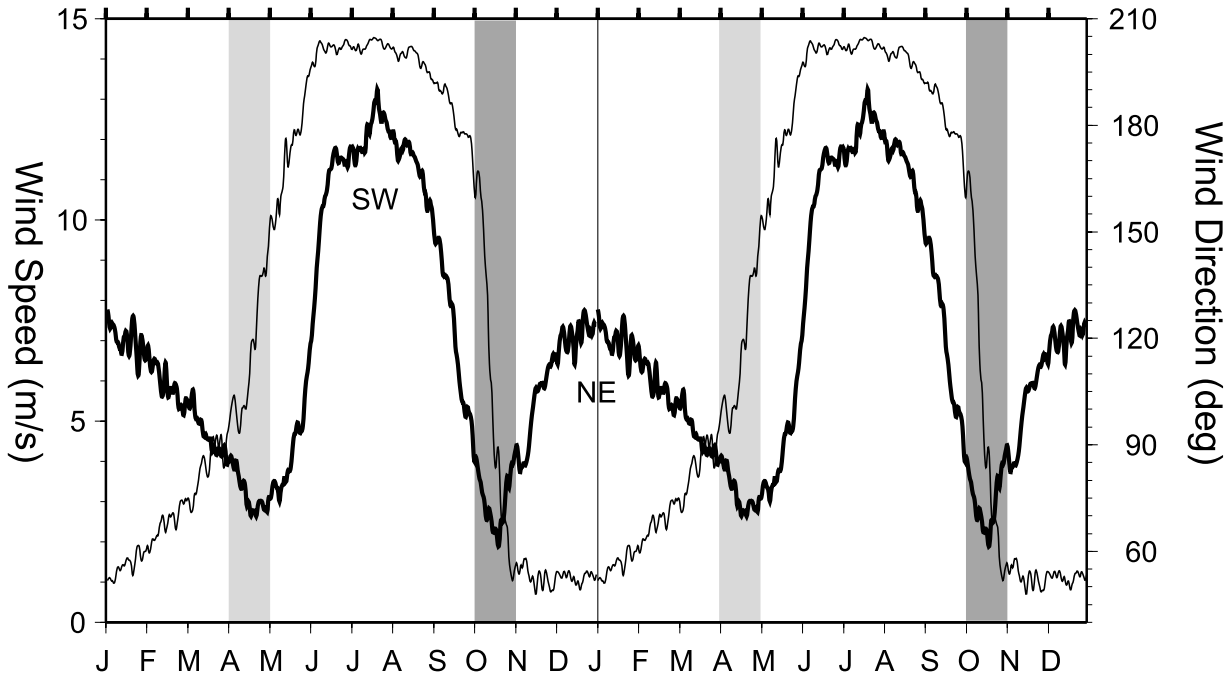

Figure 2. Climatological wind speed (thick line) and direction (thin line) near the island of Socotra in the eastern Gulf of Aden. Daily mean values are derived from an NCEP reanalysis climatology beginning in 1948 [*Kalnay et al.*, 1996]. Annual cycle is repeated for clarity. Velocity maxima associated with the southwest (SW) and northeast (NE) monsoons are highlighted. April and October monsoon transition periods are indicated by light and dark shading, respectively.

methods used and present satellite-derived evidence for ring generation in the eastern GOA. In section 3 we examine available in situ measurements and describe the ring's subsurface hydrographic and velocity structure. In section 4 we combine satellite and in situ measurements to demonstrate a relationship between Socotra Passage transport variability and ring generation. In section 5 we discuss Somali Current rings in the context of other eddy-like processes in the region and compare their characteristics with rings elsewhere in the global ocean. Our conclusions and some suggestions for future research are summarized in section 6.

2. Satellite-Derived Observations of Ring Generation

2.1. Data and Methods

[6] Rings shed by subtropical boundary currents (e.g., the Gulf Stream, Kuroshio, Agulhas Current, East Australian Current) are often discernable in satellite infrared imagery because of the contrast between their (warm or cold) core temperature and that of the surrounding environment [e.g., *Brown et al.*, 1983]. In the western Indian Ocean wind-forced coastal upwelling results in wedges and streamers of cool, nutrient-rich water which are advected alongshore and offshore by the Somali Current and its recirculations [e.g., *Evans and Brown*, 1981; *Schott*, 1983]. Although sea surface temperature (SST) imagery has been used successfully to infer aspects of the circulation in this region [e.g., *Brown et al.*, 1980], the relatively small lateral temperature gradients in the GOA – even as depicted by modern, cloud-penetrating microwave sensors – make SST relatively ineffective for feature identification and tracking when compared to ocean color. This is because upwelling provides, in addition to cooler surface temperatures, an infusion of nutrients into the euphotic zone leading to enhanced phytoplankton productivity and elevated concentrations of chlorophyll *a* in surface waters [e.g., *McGillicuddy et al.*, 1998]. The resulting contrast between the productive coastal water and the generally lifeless water of the interior Indian Ocean are visible from earth orbit using imagery from, for example, the Sea-Viewing Wide Field-of-view Sensor (SeaWiFS). Gradients in ocean color are useful for describing mesoscale ocean circulation and, in particular, the motion and evolution of isolated vortices [e.g., *Fratantoni and Glickson*, 2002].

[7] For this investigation we obtained daily fields of SeaWiFS Level 3 chlorophyll *a* data at nominal 9 km resolution for the period September 1997 to April 2004. The sole use of SeaWiFS imagery in the present study is for identification of near-surface property gradients: Our interpretation does not substantially depend on the details of instrument calibration. Further details regarding the SeaWiFS instrument, calibration methodologies, and data processing are given by *Hooker et al.* [1992] and *McClain et al.* [1998]. The western tropical Indian Ocean is frequently obscured by clouds because of intense convection associated with the monsoons and the migrating intertropical convergence zone. To minimize the impact of occasional cloudiness on our ability to discern mesoscale structures we constructed a sequence of overlapping 7-day composite images centered every fourth day and used this sequence as the basis for our analysis. Comparisons between daily and 7-day composite images during cloud-free periods indicated that temporal smearing of translating features was generally minor. A similar approach was successfully employed by *Fratantoni and Glickson* [2002] to investigate the generation and evolution of North Brazil Current (NBC) rings in the western tropical Atlantic Ocean.

[8] Satellite altimeters enable measurement of the time-varying sea surface and its spatial derivatives and thus an estimate of the geostrophic velocity field. To provide velocity information to complement the more qualitative ocean color measurements, we obtained fields of sea level anomaly (SLA; sea surface height relative to a long-term mean) temporally and spatially interpolated to 7-day, 1/3 degree Mercator grids using an objective mapping procedure. These fields, generated and quality controlled by AVISO (http://www.aviso.oceanobs.com) are a composite of measurements made by several satellite missions including TOPEX/Poseidon, GFO, Jason-I, ERS I/II, and ENVISAT. Details of the altimetric measurements and data processing procedures are described by *Ducet et al.* [2000] and *Le Traon and Dibarboure* [1999]. The SLA fields were linearly resampled to a uniform 0.25 degree grid using Delauney triangulation [*Shewchuck*, 1996] prior to analysis and velocity anomalies were computed from the gridded SLA fields assuming geostrophic balance.

2.2. Evidence for Generation of Translating Rings in the Eastern Gulf of Aden

[9] The ocean color images and SLA fields were visualized in combination using computer animation techniques. Examination of these animations revealed both the existence and the motion of numerous mesoscale vortices in the eastern GOA. Most notable were anticyclonic rings periodically generated north of the Socotra Passage. Time sequences illustrating two examples of ring generation and subsequent westward translation are shown in Figures 3 and 4.

[10] In the first image of each sequence a narrow (75–100 km) jet of low-chlorophyll Indian Ocean/Somali Current water extends northward to the coast of Yemen from the Socotra Passage, a 1000 m deep gap between the island of Abd al Kuri and the Somali peninsula. The Socotra Passage jet curves sharply to the east and south (anticyclonically) in a tight meander reminiscent of the Agulhas [e.g., *Gordon et al.*, 1987] and NBC [e.g., *Johns et al.*, 1990] retroflections. Similar flow patterns have been observed by *Molinari et al.* [1990] and *Fischer et al.* [1996], and previous synoptic surveys and numerical simulations [*Simmons et al.*, 1988] indicated an anticyclonic recirculation north of the Socotra Passage associated with the retroflecting jet. The exciting new result facilitated by joint analysis of ocean color and altimetry is the observation that the retroflecting jet periodically collapses upon itself to yield an anticyclonic vortex which translates slowly westward into the GOA. This sequence of events described above is summarized by a collage of frontal tracings in Figure 5. We observed this process a total of six times over seven years with ring formation occurring annually during boreal autumn. Three of the rings were tracked using a combination of ocean color imagery and satellite altimetry for periods exceeding 4.5 months while they translated as far west as 46°E. At

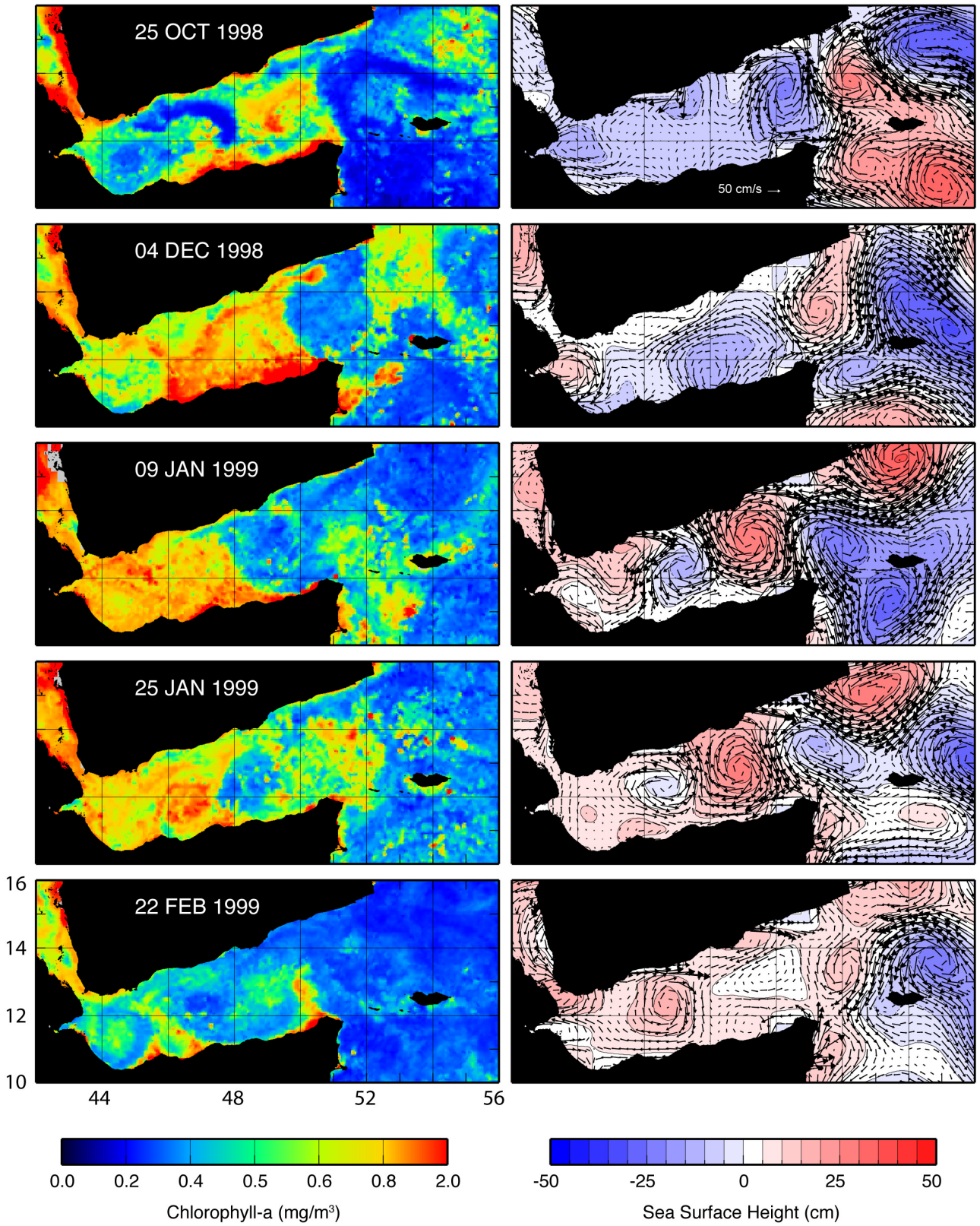

Figure 3. Time sequence of (left) remotely sensed surface chlorophyll and (right) surface height anomaly (indicated by color) and geostrophic velocity anomaly (indicated by vectors) for the period 25 October 1998–22 February 1999 illustrating the formation and westward translation of an anticyclonic ring. The cores of the anticyclonic rings are composed of relatively lifeless Somali Current water while the surrounding Gulf of Aden is relatively productive. The rings can also be tracked as a relative high in sea level anomaly.

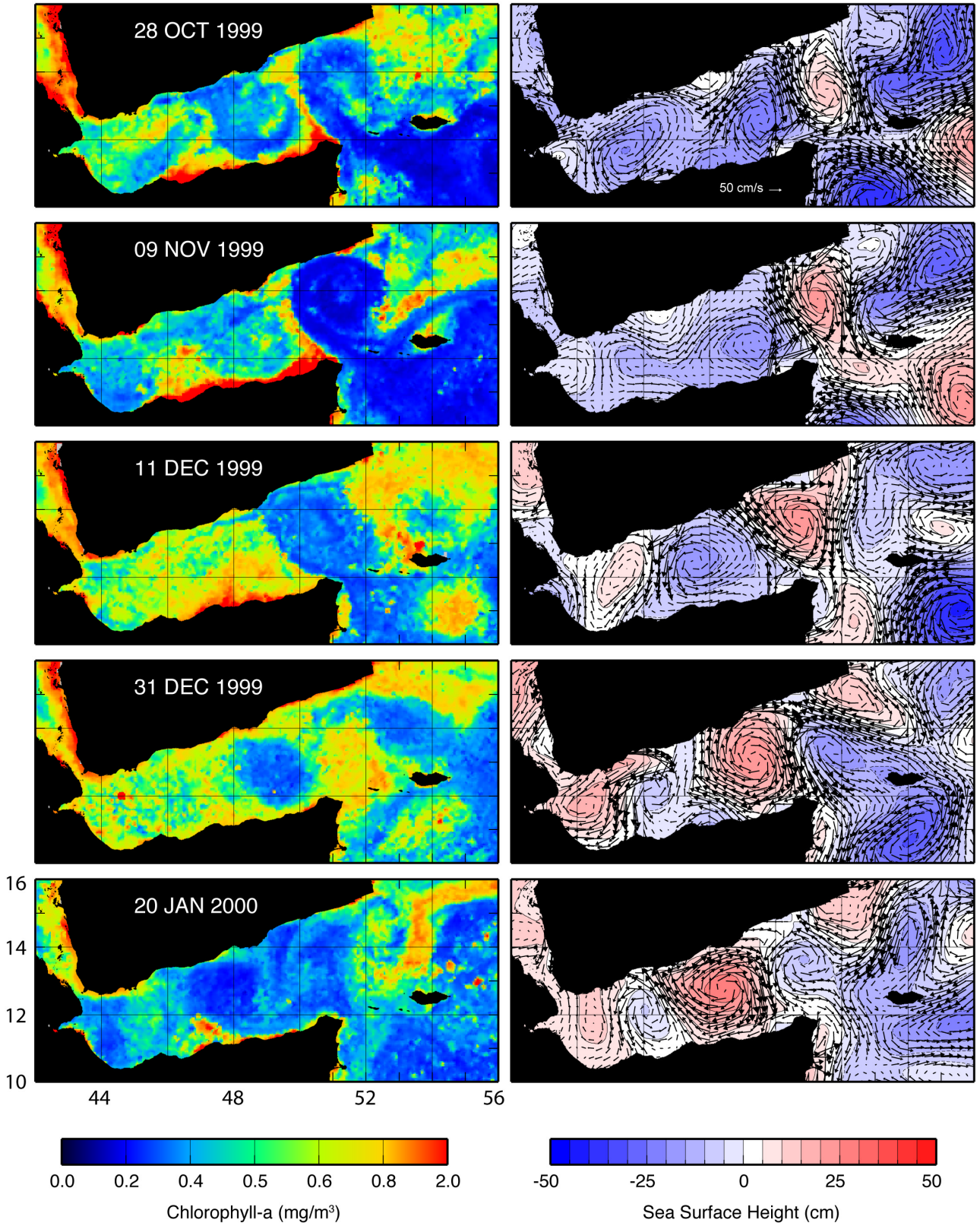

Figure 4. As in Figure 3, but for the time period 28 October 1999–20 January 2000.

this longitude the western limb of the ring's overlapped the shoaling topography east of the Bab al Mandeb.

[11] An overview of the characteristics of observed and inferred ring generation events identified during this study are provided in Table 1. Ring generation was observed each year during the first half of November with two notable exceptions: (1) Ring generation in autumn 2000 (event 4) was delayed by approximately 6 weeks until late December,

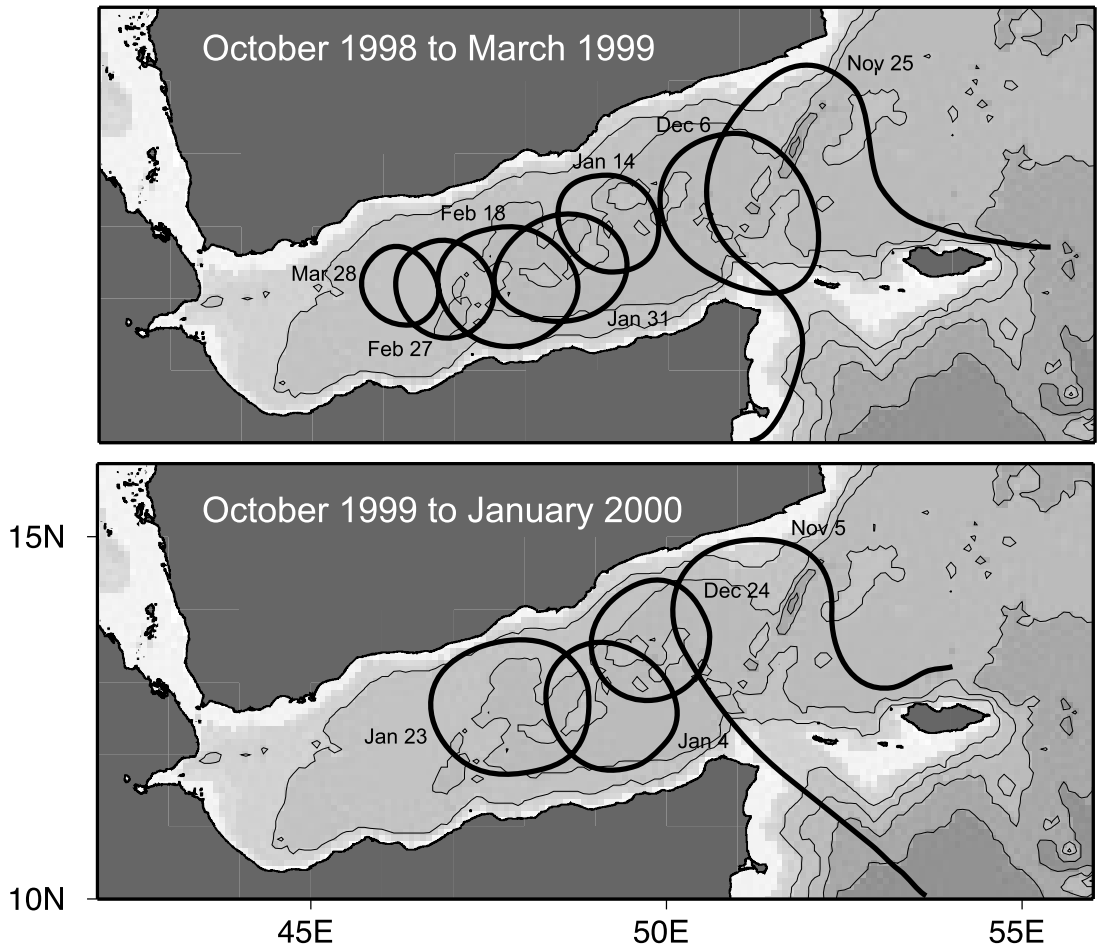

Figure 5. Frontal tracings subjectively derived from SeaWiFS chlorophyll imagery illustrating the westward translation of rings generated in early November 1998 and 1999. The retroflecting jet flowing northwards through the Socotra Passage collapses, pinching off an anticyclonic ring. The rings subsequently translate to the west at 5–8 cm/s. The ring formed in October 1998 was identifiable for more than 5 months.

and (2) ring generation was entirely absent in 2001. On the basis of the data available we cannot determine if the "missing" event in 2001 indicates absence of the process or simply our inability to detect a clear signal using remote sensing tools. The retroflecting jet and initial ring separation are most clearly illustrated by the ocean color imagery because of the high contrast in surface chlorophyll concentrations. As the ring translates westward this contrast is diminished, presumably because of a combination of local productivity and surface Ekman transport. Conversely, the velocity anomaly signature of the retroflecting jet is somewhat muddled in the eastern GOA while the anticyclonic circulation associated with the translating rings in the central gulf is quite clear.

[12] Because of periodic heavy cloud cover (particularly during July) ring formation during other times of the year cannot be ruled out. In fact, a retroflecting Socotra Passage jet was clearly observed in surface chlorophyll fields in May 2000 but it was impossible to directly observe a ring generation event because of clouds. Satellite SLA fields in June–August nevertheless show clear evidence of a westward translating ring with size and velocity properties nearly identical to the November rings. This feature, labeled "M" in Table 1, is inferred to have been generated following the April transition preceding the southwest monsoon. Additional observations of retroflecting jets and

Table 1. Observed Ring Generation Events[a]

Event	First Observed	Last Observed	Days Observed	Comment
1	11 Nov 1997	26 Jan 1998	76	strong RE
2	18 Nov 1998	06 Mar 1999	108	
3	05 Nov 1999	29 Mar 2000	144	strong RE
M	08 May 2000	24 Aug 2000	108	jet and ring observed
4	30 Dec 2000	11 Mar 2001	71	formed very late no visible ring in 2001
5	09 Nov 2002	26 Mar 2003	137	strong RE
6	04 Nov 2003	24 Mar 2004	140	

[a]Ring generation was generally observed in boreal autumn of each year except for 2000 and 2001. Ring formation in May 2000 (M) is inferred from independent observations of a retroflecting jet and a translating vortex, but the actual generation event was not witnessed. The 2000–2001 November ring (event 4) occurred unusually late in the year. Recirculation eddies (RE) on the eastern flank of rings were particularly notable in 1997, 1999, and 2002 (events 1, 2, and 5).

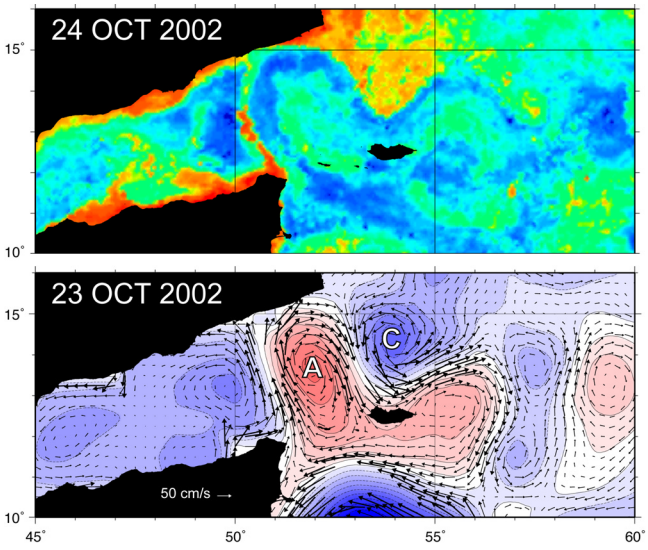

Figure 6. A particularly clear example of the retroflecting Socotra Passage jet. Note the development of a cyclonic recirculation to the east of the anticyclonic retroflection associated with the meridional overshoot of the meandering current. Anticyclone (A) and cyclone (C) eventually move westward together into the Gulf of Aden.

ring generation in May of other years are highly suggestive but sufficiently impacted by clouds and/or low-chlorophyll contrast to be inconclusive. (This situation was not substantially improved by reviewing cloud-penetrating microwave radiometer imagery because of both limited resolution and weak horizontal gradients (M. Caruso, personal communication, 2003).) We will demonstrate in section 4, below, that inferred flow conditions in Socotra Passage during May and November support the notion that ring generation events occur twice per year and are generally correlated with the monsoon transitions.

2.3. Ring Characteristics

[13] The observed rings are comparable in overall diameter to the width of the GOA (220 km), exhibit azimuthal velocities greater than 50 cm/s, and move westward into the gulf at 5–8 cm/s. Length scales inferred from the ocean color measurements correspond well to radii of maximum velocity estimates (80–100 km) determined from altimetric measurements and in situ estimates (see section 3). *Fratantoni and Glickson* [2002] previously demonstrated that the surface chlorophyll front associated with a mesoscale ring is approximately colocated with the radius of maximum azimuthal velocity. Additional support for this claim is provided by a comparison with surface drifter trajectories illustrated in Figure 12 in section 4.

[14] Note that geostrophic velocity anomalies computed from SLA fields likely underestimate the true azimuthal circulation because of the neglect of inertial components of the momentum balance and smoothing inherent in the mapping of the SLA fields [see, e.g., *Didden and Schott*, 1993]. Inertial effects undoubtedly play a large role in ring generation, and particularly in the high-velocity flow near and through the narrow Socotra Passage. The geostrophic velocity anomaly field in, for example, Figure 6, certainly underestimates the true flow field as it takes into account neither the mean circulation through the Socotra Passage nor that associated with the Socotra Gyre. Absolute velocity estimates from shipboard acoustic Doppler current profiler (ADCP); [e.g., *Fischer et al.*, 1996] indicate recirculating near-surface velocities in the Socotra Gyre exceeding 150 cm/s, or almost twice the velocity amplitude shown in Figure 6.

2.4. Cyclonic Recirculation Eddies

[15] In at least three of the six observed ring generation events a cyclonic recirculation eddy was observed to spin up adjacent to and east of the newly formed anticyclonic ring. These cold-core eddies form in a recirculation induced by the meridional overshoot of the retroflecting Socotra Passage jet (Figure 6). *Simmons et al.* [1988] report similar cold-core features in both synoptic expendable bathythermograph (XBT) surveys and numerical simulations, but regard them as seasonally modulated stationary features rather than translating eddies. The cyclonic recirculation eddies do not have a strong chlorophyll gradient signature but are discernable in the SLA and geostrophic velocity fields. The recirculation eddies are of comparable scale to the anticyclonic rings and the ring-eddy pairs appear to move westward together as a unit. While this process (Figure 7) may contribute to the pattern of counterrotating vortices observed to fill the GOA during recent in situ hydrographic and direct velocity surveys [e.g., *Bower et al.*, 2002], the ring-eddy pairs translate westward too slowly to maintain this pattern throughout the year.

[16] On the basis of remote observations of a limited number of rings it appears that the anticyclonic rings have stronger azimuthal velocities and persist somewhat longer than the cyclonic recirculation eddies. We observed numerous instances in which adjacent, counterrotating vortices interacted with each other. Such interactions occasionally resulted in a reversal in translation direction with an

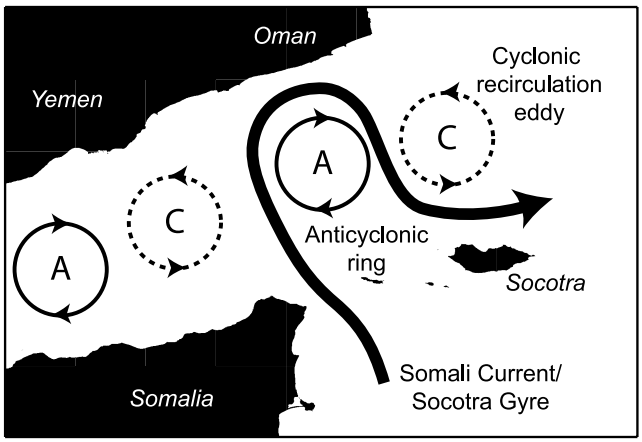

Figure 7. A schematic depiction of the observed ring formation mechanism. Anticyclonic rings are wrapped-up pieces of Somali Current which pinch off from the retroflection near the mouth of the Gulf of Aden. Cyclonic recirculation eddies spin up within a cyclonic current meander to the east of the retroflection and are not necessarily encapsulated by Somali Current water.

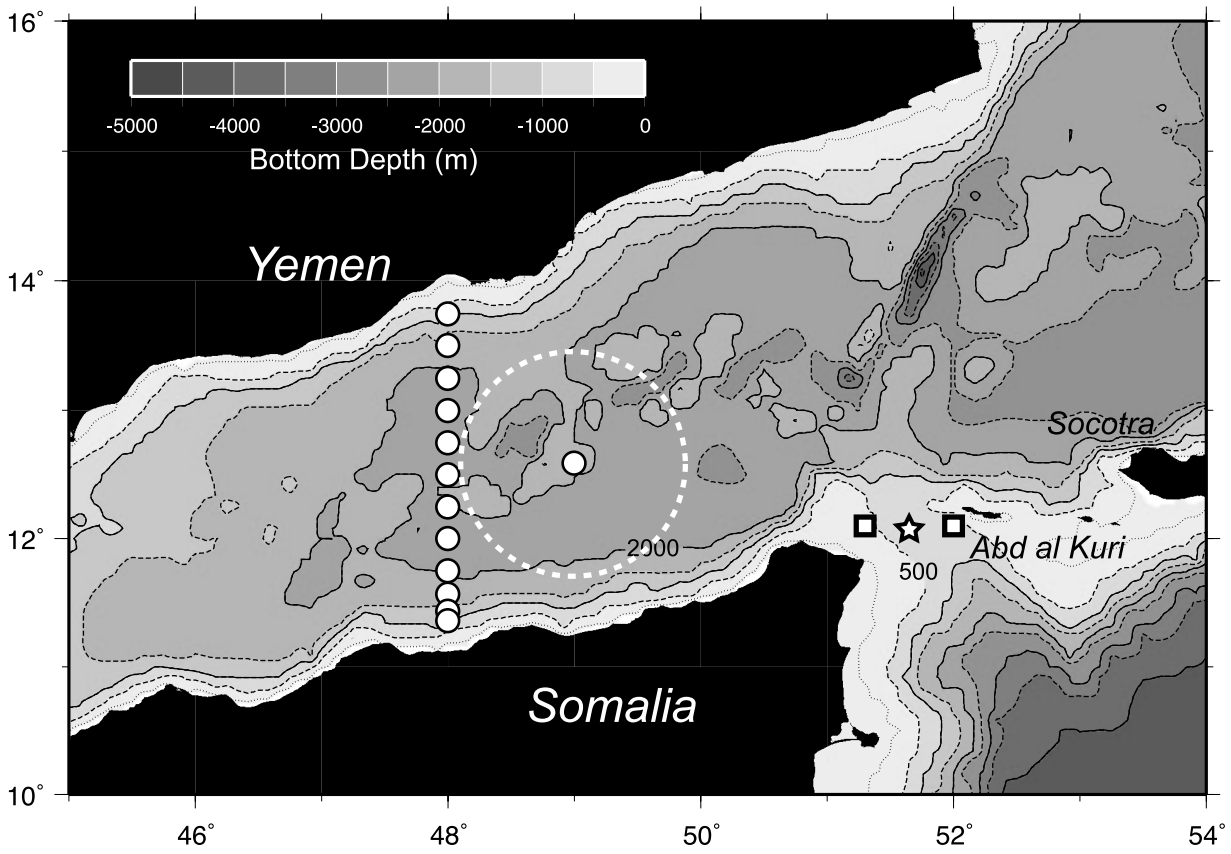

Figure 8. Bathymetry of the eastern Gulf of Aden. Location of conductivity, temperature, depth (CTD) stations used in the hydrographic sections of Figure 9 are indicated with circles along 48°E. Satellite imagery indicated that CTD 226 at 49°E, 12.5°N was close to the center of a ring with a 100 km radius of maximum velocity (dashed circle). Location of current meter mooring K10 in the Socotra Passage [*Schott et al.*, 1997] is indicated with a star. Squares indicate the locations at which sea level anomaly time series were extracted for the model developed in section 4.

anticyclonic ring moving eastward toward the mouth of the GOA.

3. In Situ Observations

3.1. Hydrographic Measurements

[17] Temperature, salinity, dissolved oxygen, and absolute velocity measurements were collected on a total of 462 hydrographic stations occupied during regional cruises in February–March and August of 2001. Treatment of the hydrographic and velocity data are summarized by *Johns et al.* [2001] and *Peters and Johns* [2006], respectively. On the basis of postcruise analysis of satellite imagery and ship-based direct velocity measurements [*Bower et al.*, 2002] we determined that a March 2001 meridional section along 48°E (see Figure 8) partially transected an anticyclonic ring generated in December 2000 (our event 4; see Table 1). It does not appear that this section passed through the center of the ring but rather sliced through the ring's western limb at a distance of 75–100 km from the center.

[18] Cross sections of several hydrographic variables plotted along this meridional section are shown in Figure 9. Clearly evident are the elevated salinity and oxygen signatures associated with the Red Sea outflow between 500 and 1000 m depth, and a relatively fresh, relatively high oxygen layer just below the main thermocline indicative of Somali Current water originating near the equator. Near 200–250 m depth there is a hint of accentuated salinity and oxygen properties within the ring core, but the scale of the anomalous region and the property values themselves are skewed because of the offset of the section nearly one radius of maximum velocity west of the ring center. The azimuthal velocity section indicates an anticyclonic circulation with maximum velocities near 40 cm/s at 250 m depth. The ring is capped at the surface by a 100–150 m thick layer of westward flow consistent in sign with Ekman transport driven by the northeasterly winds. As previously reported by *Bower et al.* [2002] there is a barotropic component of the ring circulation. The vortex extends coherently to at least the top of the local ridge crests (1500 m) and perhaps all the way to the bottom.

[19] The water properties in the ring's core are better evaluated using a single hydrographic station located about 100 km east of the previous section and somewhat closer to the actual ring center (see Figure 8). The vertical water mass structure of the ring can be compactly summarized by a collection of salinity-oxygen diagrams constructed on constant potential density surfaces (Figure 10). The isopycnal

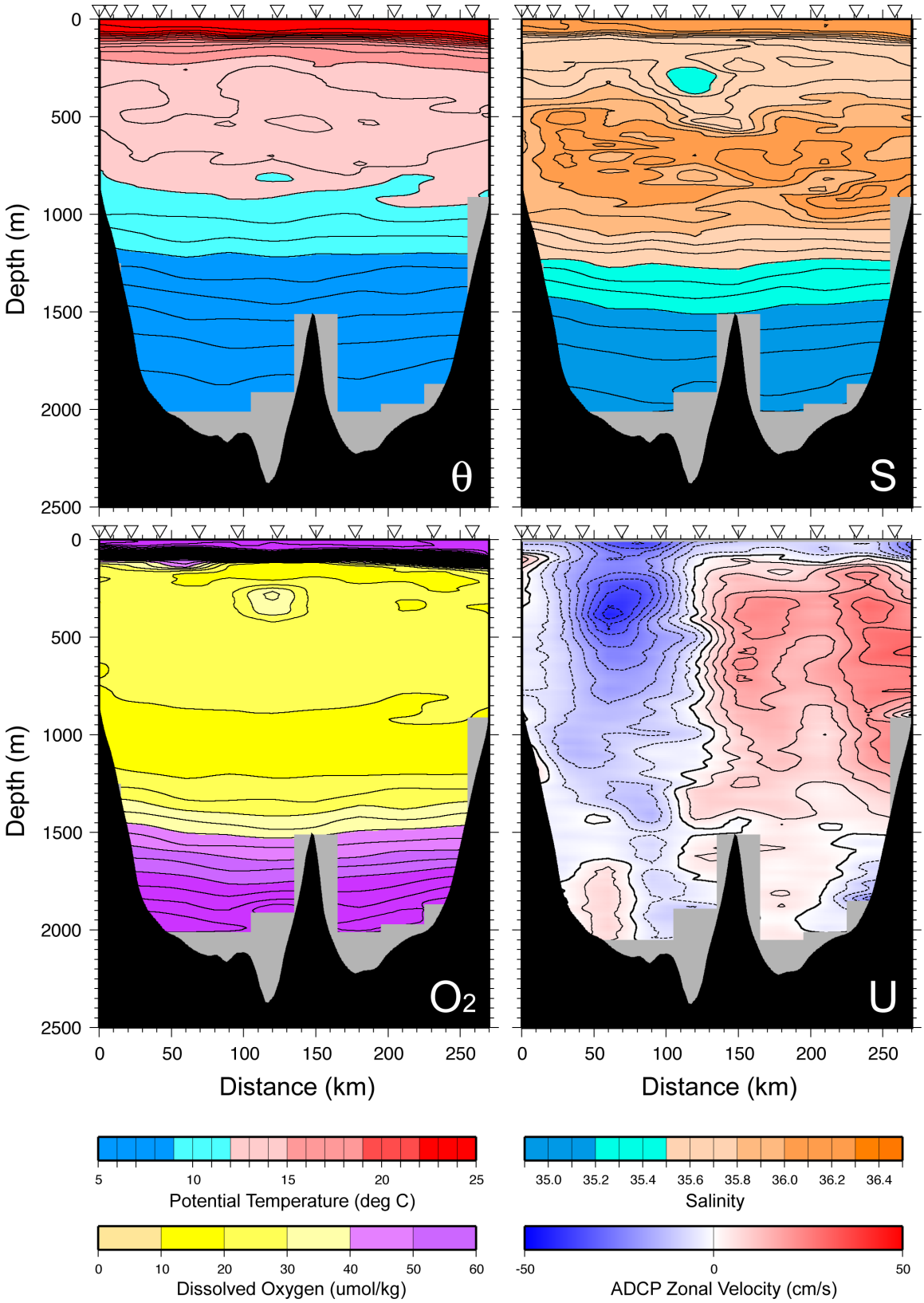

Figure 9. Hydrographic section occupied along 48°E in March 2001. Distance is measured northward along the section. Station locations are indicated by inverted triangles. Velocity section is based on lowered acoustic Doppler current profiler measurements [see *Peters and Johns*, 2006]. Contour intervals are 1°C for temperature, 0.1 for salinity, 5 umol/kg for dissolved oxygen, and 5 cm/s for zonal velocity (positive eastward).

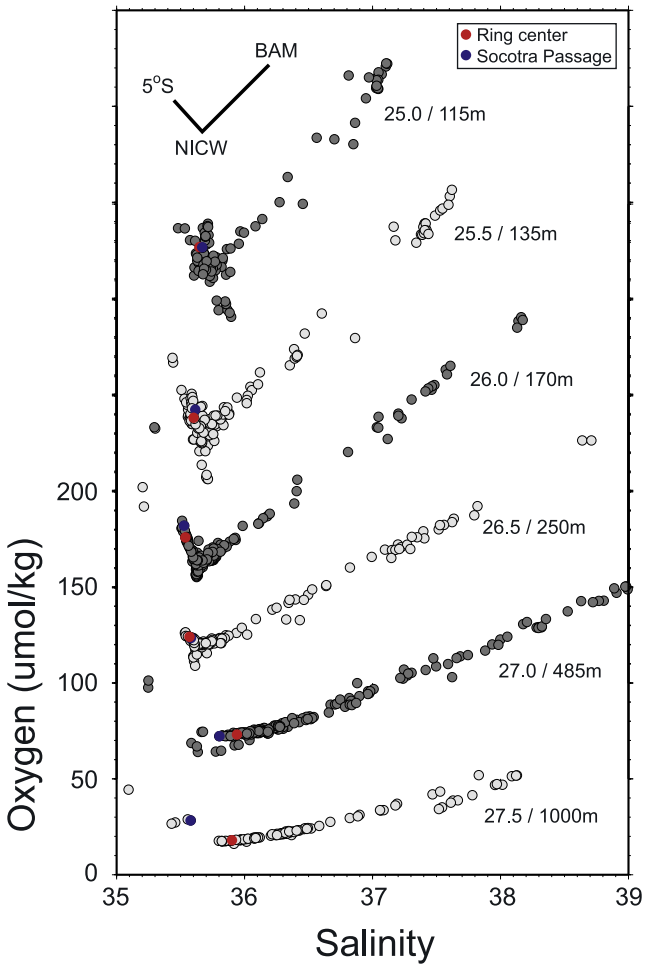

Figure 10. A summary of the isopycnal relationship between salinity and dissolved oxygen based on stations occupied in the Gulf of Aden (GOA) in February–March 2001 [see *Johns et al.*, 2001]. Density surfaces and approximate depths (in the eastern GOA) are indicated. For clarity each S-O_2 relation is offset vertically by an arbitrary constant. Two stations in the inferred center of an anticyclonic ring (CTD 226) and in the Socotra Passage (CTD 236) are highlighted.

salinity-oxygen relationship in this area of the world has a characteristic shape in the upper ocean resulting from several competing processes. The highest salinities at all depths are found near the Bab al Mandeb where the Red Sea outflow enters the western GOA. The removal of oxygen from the water column by respiration in the biologically active Arabian Sea results in the lowest oxygen values [e.g., *Broecker and Peng*, 1982; *Olson et al.*, 1993] and the lowest salinities are found in waters of equatorial origin.

[20] Figure 10 indicates that hydrographic properties at depths from the surface through the azimuthal velocity maximum are nearly identical to those measured within the Socotra Passage, indicating that the ring's most intense circulation is consistent with a wrapped-up piece of the equator-crossing Somali Current. As will be shown in greater detail, the strongest northward flow through Socotra Passage is generally isolated above 200–300 m and decays rapidly with depth [*Schott and Fischer*, 2000]. Below 400 m depth the water mass properties depart from those in Socotra Passage and are more consistent with water found in the Arabian Sea. The apparent difference in origin of near-surface versus deep layers within the ring is consistent with the observed vertical structure of velocity in both the ring and the Socotra Passage. While the ring may be initially formed from a wrapped-up piece of the (shallow) Socotra Passage jet, there is clearly a barotropic aspect of the resulting vortex evident in the cocirculation of water at greater depths (Figure 10).

[21] One simple dynamical explanation for this observation invokes potential vorticity (PV) conservation in a two-layer system [see, e.g., *Cenedese and Whitehead*, 2000]. As the upper-layer Socotra jet invades the northern GOA and curves back on itself the depressed thermocline associated with the resultant anticyclone compresses the previously quiescent lower layer. PV conservation requires that anticyclonic relative vorticity be generated in the lower layer. Symbolically, PV = (f/H) = (ζ + f/H − η) where H is the lower layer depth, η the thermocline depression, ζ the lower layer vorticity, and F the Coriolis parameter. Reasonable approximations for H (2000 m) and η (100 m) yield a required anticyclonic vorticity in the lower layer of magnitude 1.6×10^{-6} s^{-1}. The observed vorticity in the lower layer eddy core can be roughly approximated as u/R, where u is the lower layer azimuthal velocity and R is the radius of maximum velocity. Assuming u and R of 15 cm/s and 100 km, respectively, yields a lower layer relative vorticity within 10% of the theoretical expectation. Thus it seems entirely possible for the relatively shallow Socotra jet to result in a ring with a deep reaching coherent circulation yet vertically disparate water mass origins.

3.2. Surface Drifters

[22] In an attempt to further confirm the origin of the ring core water we searched the National Oceanic and Atmospheric Administration (NOAA) Global Drifter Archive (http://aoml.noaa.gov) for all satellite-tracked surface drifters in the eastern Gulf of Aden. Unfortunately there were few drifters in this area of the world, and still fewer that exhibited ring- or eddy-like looping behavior. Four illustrative examples from 1995 to 1997 are shown in Figure 11. Drifter 19161 (Figure 11a) entered the GOA from the northeast along the Arabian peninsula before becoming entrained in a cyclonic eddy that translated westward over a period of 3 months. On the basis of the location at which the looping began we speculate that this eddy is similar in origin to the recirculation eddies described above. The remaining three drifters in this figure all entered the eastern GOA through the Socotra Passage. Drifters 21889 and 21859 each looped once before leaving the area (Figures 11b and 11c). Drifter 21889 performed an anticyclonic loop in May during the period associated with the unusual ring generation event "M" described above. Drifter 21859 performed a cyclonic loop in roughly the same position and at the same time of year as 19161. Drifter 21843 in Figure 11d looped anticyclonically while translating westward south of Socotra, passed through the Socotra Passage, and then looped cyclonically several times north of Socotra before heading east into the Arabian Sea. None of

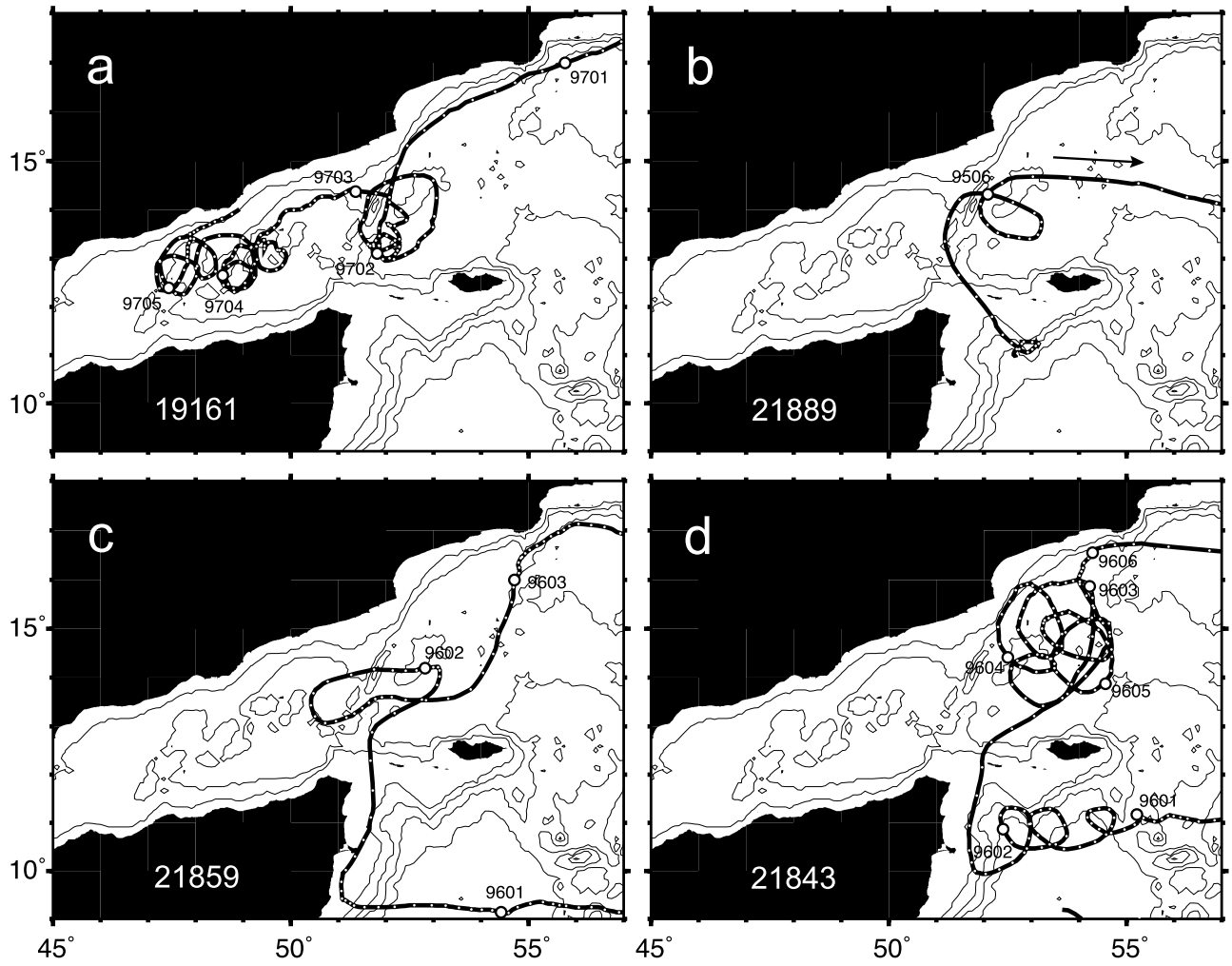

Figure 11. Trajectories of four surface drifters obtained from the NOAA Global Drifter Archive. Drifter position is indicated each day (small dot) and month (large dot with date: YYMM).

these drifters depict the formation of a Somali Current ring as described in the previous sections but this is probably because of the small number of drifters available, none of which were appropriately located during the November time frame when formation events are most clearly evident in the satellite observations.

[23] Three acoustically tracked subsurface RAFOS floats used to track the Red Sea outflow (see *Bower et al.* [2005] and *Furey et al.* [2005] for details) completed their missions and ascended to the surface within an anticyclonic eddy in September 2002. The surface drift of these floats is plotted in Figure 12 along with a SeaWiFS composite image associated with the approximate temporal midpoint of the trajectories. The float trajectories are each several weeks in length. Because of intense cloudiness in the preceding months we cannot confirm that the feature illustrated is a ring generated in the manner described in section 2. Regardless, these trajectories clearly illustrate the relationship between the near-surface circulation and satellite-derived surface chlorophyll distribution. Azimuthal velocities of 25–35 cm/s were measured in the anticyclone by the drifting RAFOS floats before all three eventually grounded on the coast of Yemen.

4. Ring Generation and Socotra Passage Transport

[24] The remotely sensed observations described in section 2 suggest a relationship between ring formation in the eastern GOA and enhanced northward upper ocean transport through the Socotra Passage in the form of a retroflecting jet. In particular, the generation of rings following the October monsoon transition and the scarcity of generation events at other times lead us to speculate that ring formation should be associated with identifiable, and perhaps annual, maxima in Socotra Passage transport.

[25] The only existing long-term measurements of Socotra Passage velocity and transport result from moored current meter measurements collected during an 18-month period in 1995–1996 as part of the World Ocean Circulation Experiment (WOCE) ICM-8 array [*Fischer et al.*, 1996; *Schott et al.*, 1997; *Schott and Fischer*, 2000]. These

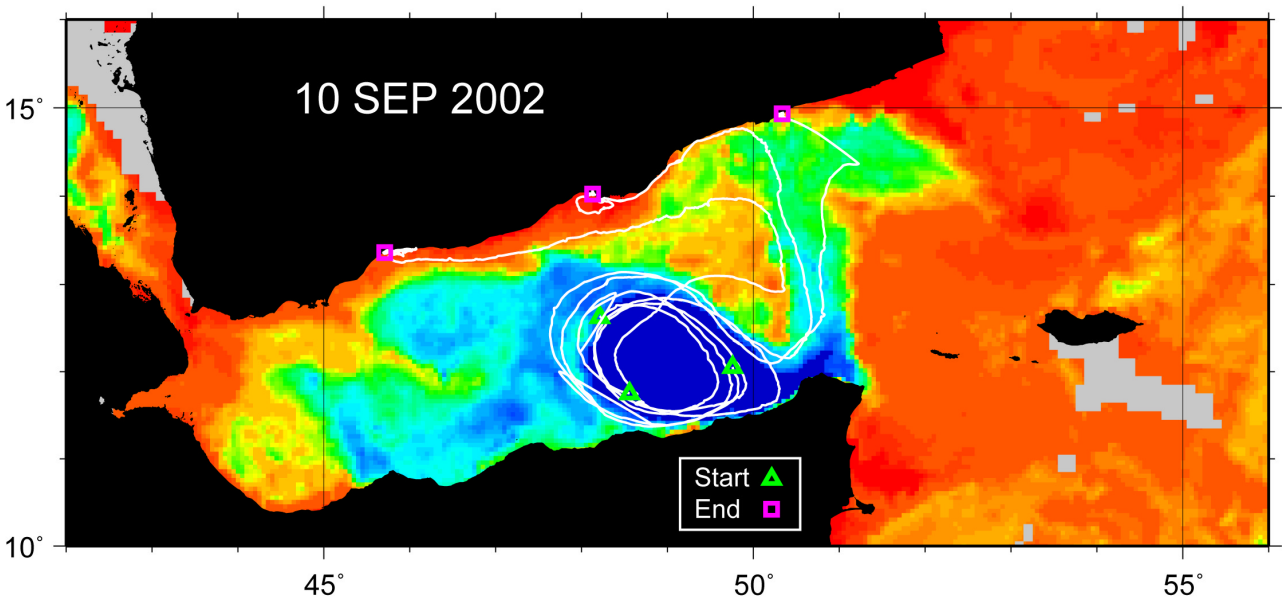

Figure 12. Trajectories of three RAFOS floats which completed their subsurface mission and surfaced within an anticyclonic feature. Each of the trajectories is 3–5 weeks in length. Background SeaWiFS chlorophyll image coincides with the approximate midpoint of the trajectories. Note the general agreement between the surface chlorophyll gradients and the surface velocity field depicted by the float trajectories.

velocity records indicate generally northward flow through the Socotra Passage with near-surface velocities exceeding 200 cm/s during the height of the southwest monsoon. *Schott and Fischer* [2000, Figure 9 and Table 1] report that on the basis of two current meter moorings, flow through Socotra Passage above 200 m is strongly northward with little horizontal variation, while below 200 m mean flow is southward on the western side of the channel and northward on the eastern side (Figure 13). To the extent that northward velocities in the upper 200 m were found to be nearly equal at each site, we can approximate the upper layer transport using the velocity measured at a single mooring location multiplied by a constant representing the cross-sectional area of the passage (Figure 14a). Most of the transport occurs in the upper 200 m with the 200–400 m layer accounting for an additional 2–3 Sv during period of peak flow. Following the October 1995 monsoon transition the inferred northward upper layer transport briefly peaked near 12–15 Sv, or roughly three times the annual mean. This transport peak is of particular relevance to this study as it coincides with the expected timeframe for onset of a boreal autumn Socotra Passage jet and subsequent ring generation. Is this peak in transport an annual event?

4.1. A Simple Model of Socotra Passage Flow Variability

[26] Unfortunately there have been no other long-term moored measurements collected in this region. We therefore developed a simple model for Socotra Passage flow variability using the only long-term time series data available: satellite altimetry. The upper layer transport through the Socotra Passage is related to the slope of the sea surface across the passage through the geostrophic relation, $v = (g/f)(dh/dx)$, where g is the gravitational acceleration, f the Coriolis parameter, and dh/dx is the slope of the sea surface in the direction normal to the velocity v. If time-dependent, inertial, and dissipative effects are assumed to be small, then direct application of this relationship should yield reasonable results for the fluctuating velocity using satellite altimetry to provide the sea surface slope information.

[27] Skeptical of these fairly restrictive dynamical assumptions applied to a narrow channel near an energetic western boundary, we developed a simple empirical model validated by the existing Socotra Passage current meter data. A single velocity time series from mooring K10 at a depth of 48 m closely approximates the upper layer passage transport computed above. For simplicity we use here the (known) velocity record rather than an (estimated) transport time series to fit the empirical model. The velocity time series (Figure 14b) was rotated in a direction parallel to the channel axis and demeaned. To facilitate comparison with the altimetric measurements the velocity anomaly time series was subsampled at 7-day intervals corresponding to the SLA observations. Most of the energy in this record is concentrated in the 40–60 day and seasonal-annual bands (not shown) thus this subsampling does not substantially compromise the fidelity of the model. A time series of SLA difference across the channel was computed from a pair of grid points near 12°N and separated by approximately 75 km (see Figure 8). Linear regression was used to determine the constant of proportionality between observed SLA difference and measured velocity anomaly (Figure 15b). Several different grid point pairs were evaluated. We found no particular sensitivity to the choice of grid points for this calculation provided the

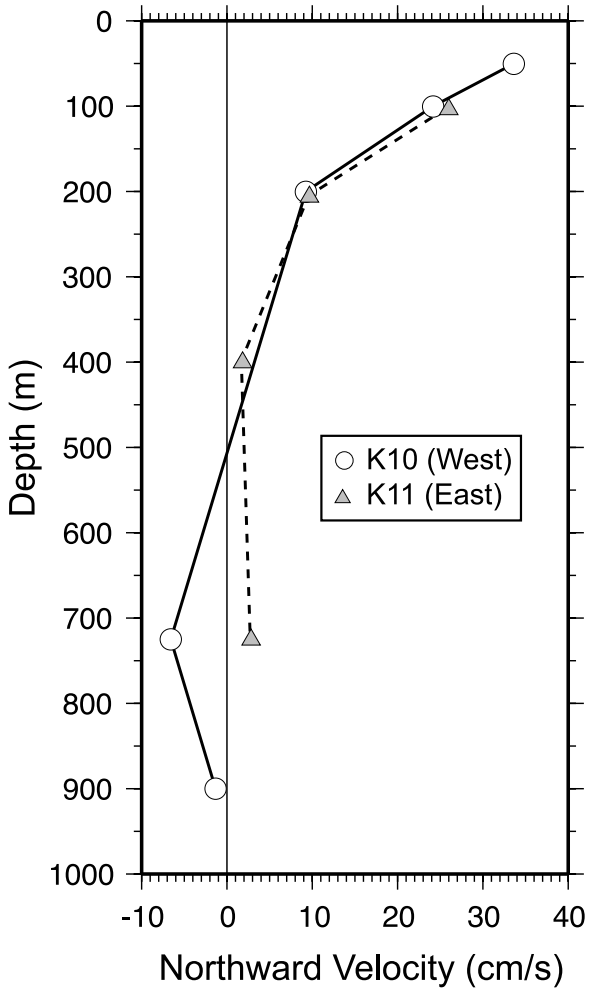

Figure 13. Record-length mean vertical structure of northward velocity in Socotra Passage during 1995–1996 based on current meter observations at moorings K10 (solid line) and K11 (dashed line) [see *Schott et al.*, 1997].

grid point pair spanned the channel and neither grid point was unreasonably close to shore.

[28] The slope of the linear fit in Figure 15a corresponds parametrically to the factor (g/fL) in the geostrophic relation, where L is the separation between discrete SLA measurements. (Note that for this simple empirical model there is no a priori reason why this relationship should be linear. The observation that it is (approximately) linear suggests that an assumption of geostrophic balance is not unreasonable.)The empirically derived slope (3.88) is within 10% of a straightforward geostrophic estimate (4.26) determined using the same pair of SLA grid points suggesting that our earlier concerns about ageostrophic effects may have been overstated. The original (subsampled and demeaned) velocity anomaly time series and the final modeled series are shown in Figure 15b. The comparison is reasonably good, with the most notable deviations during July–August when the strongest negative (southward) velocity anomalies occur. The modeled velocity misses some of the higher-frequency variability (e.g., February 1996) but captures most of the longer-period fluctuations.

4.2. Model Results

[29] Recall that our goal in constructing this simple model was to develop a means to roughly compare the timing of observed ring generation events with inferred Socotra Passage transport anomalies. The result of this effort is the multiyear time series of velocity anomaly shown in Figure 16a. It is immediately apparent from this figure that large northward velocity events in the Socotra Passage are episodic, occurring no more frequently than 2–3 times in a given year with each event lasting for no more than 2–3 months. Most importantly for the present study there appears to be an annually recurring maximum velocity event, typically in November. These surges could result from seasonal, wind-induced changes in the configuration of the Socotra Gyre, a relatively stationary recirculation of the Somali Current that appears during the southwest monsoon [e.g., *Bruce*, 1979; *Fischer et al.*, 1996]. While the exact timing of this event varies from year-to-year it is bounded between late October and early January with a mean in November. The velocity anomaly associated with a particular November peak is typically 50–75 cm/s. In most years, and in a composite annual cycle (Figure 16b) there is also a secondary velocity peak in May.

[30] With this information we are now able to demonstrate that each of the ring formation events described in section 2 can be uniquely mapped to a local maximum in Socotra Passage flow. The circled numbers in Figure 16a indicate the velocity anomalies coincident with the ring generation events summarized in Table 1. Note particularly the absence of an observed ring generation event in 2001 and the corresponding lack of a large amplitude velocity peak. Similarly, the relatively late ring generation event noted in 2000 (event 4) occurs simultaneously with a later-than-normal velocity peak. The event labeled "M" corresponds to a May 2000 observation of a retroflecting Socotra Passage jet mentioned above in section 2. Figure 16 indicates that in most years a secondary maximum in velocity occurs in May, closely following the transition period between the northeast and southwest monsoons (Figure 2). The May 2000 event is clearly of larger amplitude than any other year in the study period and this may explain why it was at least partially observed while those in other years fell below our (subjective) detection threshold.

[31] In summary, our initial speculation regarding a relationship between episodic maxima in Socotra Passage transport and ring generation events appears to be supported by the data, subject to obvious caveats related to our proxy for passage transport. To the extent that Figure 16 is representative of actual flow variability in Socotra Passage, we have also learned that ring formation during both monsoon transitions (i.e., November and May) is likely, a result we would not have predicted on the basis of satellite image analysis alone. Both the November and May velocity peaks in the Socotra Passage closely follow the rapid change in wind speed and direction associated with the transition between monsoon phases (Figure 2). This suggests a direct relationship between regional wind forcing, local flow in the Socotra Passage, and episodic mesoscale ring generation in the eastern GOA. We found no obvious correlation between passage flow and National Center for Environmental Prediction (NCEP) reanalysis winds [*Kalnay*

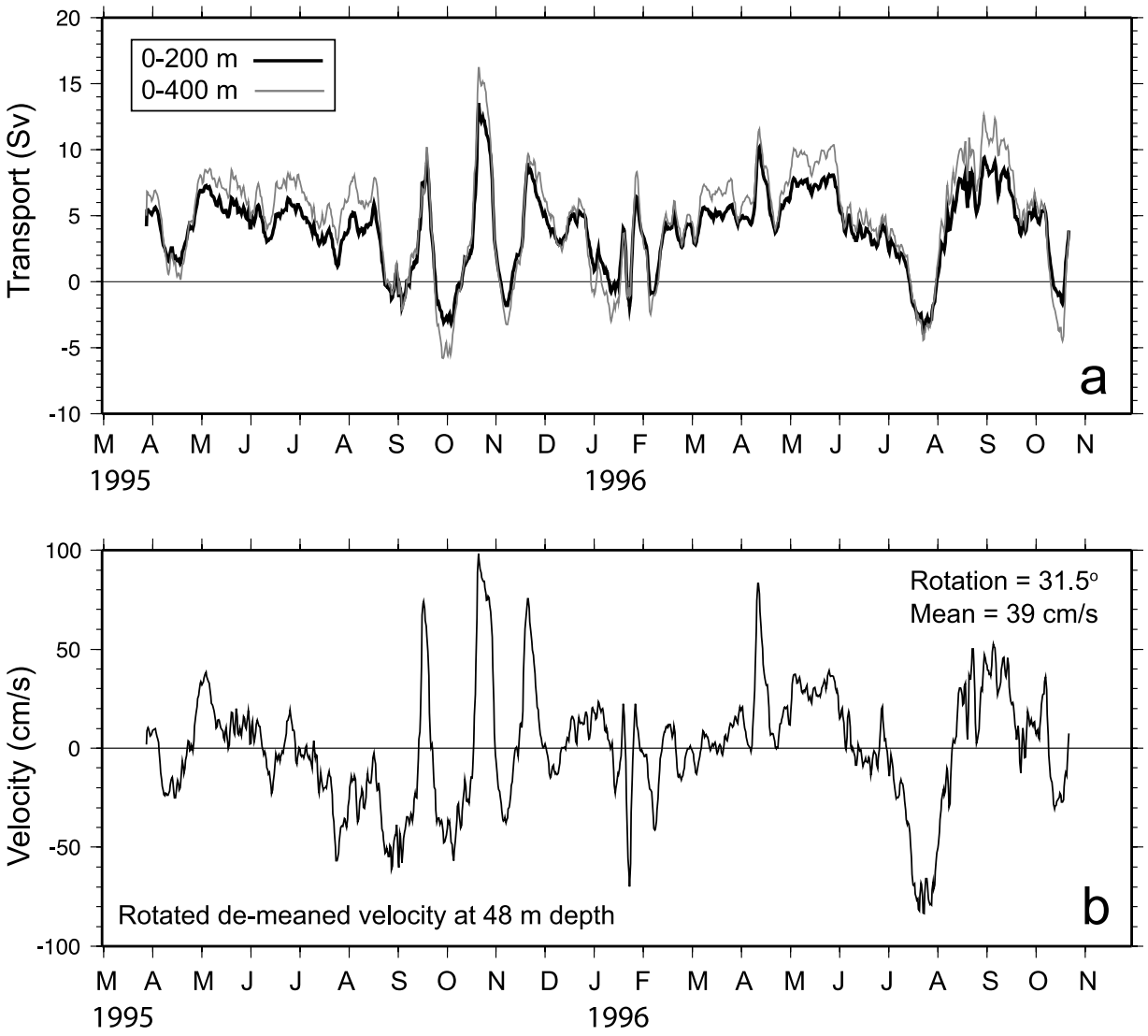

Figure 14. Transport and velocity in Socotra Passage during 1995–1996 on the basis of moored current meter observations [*Schott et al.*, 1997]. (a) Transport through Socotra Passage in the upper 200 m (bold line) and upper 400 m (grey line). For this calculation we assumed a passage width of 64 km and extrapolated upwards from the shallowest available instrument assuming no vertical shear; (b) Rotated and demeaned velocity at 48 m depth from mooring K10 (see Figure 8 for location).

et al., 1996] near the Socotra Passage suggesting that remote forcing of the western boundary current system by basin-scale wind stress curl [e.g., *Anderson and Rowlands*, 1976] plays a more important role than local wind speed.

5. Discussion

[32] A preponderance of the world's tropical and subtropical western boundary currents generate discrete, translating rings from pinched-off current meanders. In some boundary current systems (e.g., the Gulf Stream, Kuroshio, Agulhas) rings form in the open ocean and may translate for thousands of kilometers before dissipating. Elsewhere ring formation and translation are topographically constrained, and individual features may survive for only a few months (e.g., Gulf of Mexico Loop Current, North Brazil Current, and South China Sea). On the basis of observations to date, the South Equatorial/Mindanao Current system in the western tropical Pacific [*Lukas et al.*, 1991] now appears to be the only major tropical or subtropical western boundary current system that does not exhibit ring shedding of some form. Whether this distinction is due to lack of observations or to underlying dynamical constraints [e.g., *Nof*, 1996] remains to be confirmed. (The numerical models of *Qiu et al.* [1999] and *Matsumoto et al.* [2001] suggest the existence of westward propagating intraseasonal eddies in the Sulawesi Sea. We are as yet unaware of any observational verification of these features.)

[33] The Somali Current rings described herein appear to be quite similar in structure and behavior to rings shed by western boundary currents elsewhere in the global ocean, even though they are among the lowest latitude and most topographically constrained (see *Olson* [1991] for a review). For example, the generation mechanism and ultimate struc-

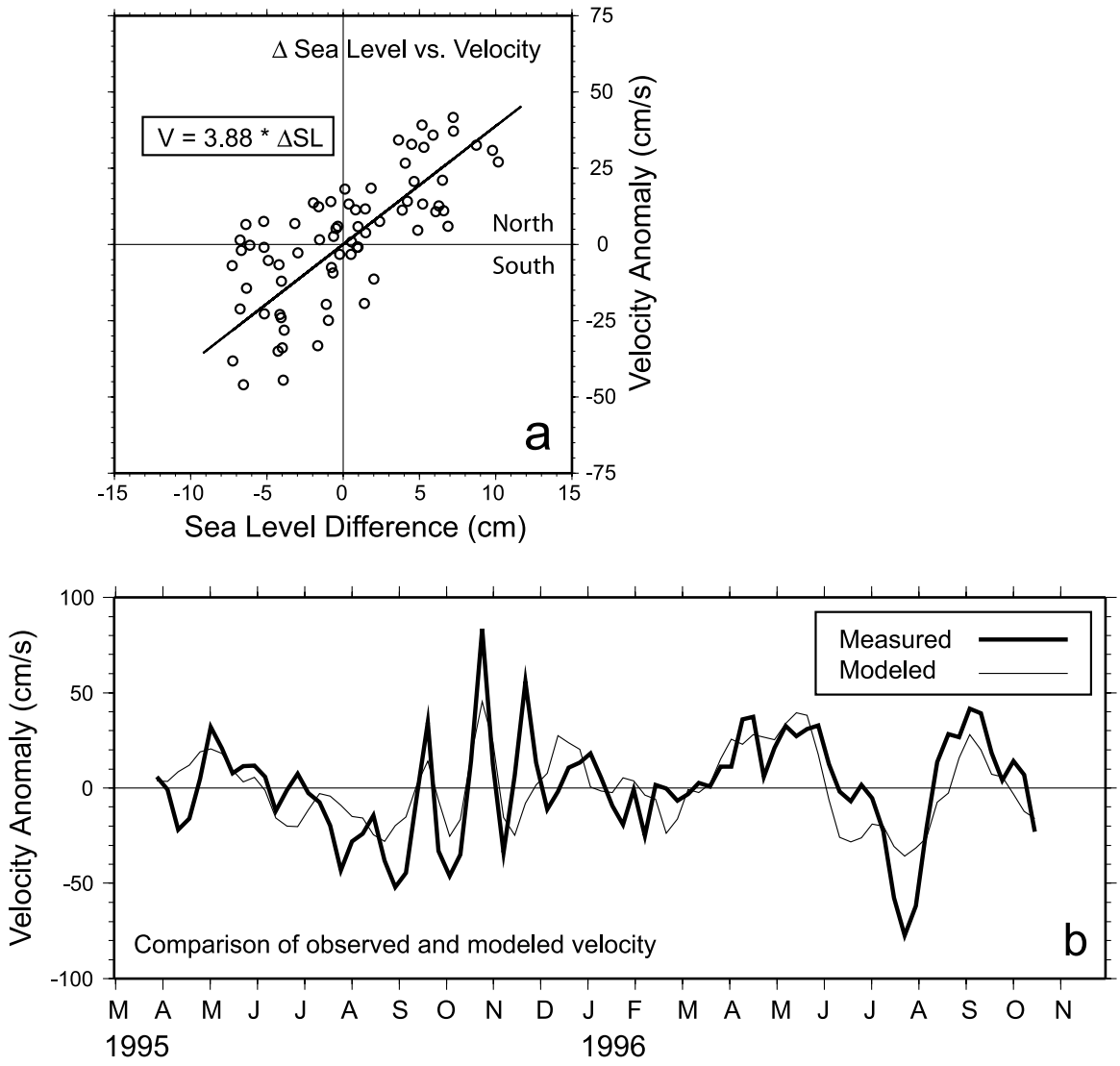

Figure 15. (a) Correlation between sea level difference across the Socotra Passage and a subsampled version of the measured velocity anomaly at 48 m from mooring K10. A linear relationship is assumed to model velocity anomaly as a function of sea level difference; (b) Comparison of observed and modeled velocity time series.

ture of the Somali rings appears most similar to the anticyclonic rings formed in the western tropical Atlantic by the retroflecting NBC [e.g., *Johns et al.*, 1990; *Fratantoni and Glickson*, 2002; *Fratantoni and Richardson*, 2006]. Although the basic formation mechanism and physical characteristics of these low-latitude rings are similar, their interactions with the general circulation and regional topography differ substantially. NBC rings are generated at a rate of 8–9 per year [*Johns et al.*, 2003] and are slightly larger than those in the GOA with a typical radius of maximum velocity near 125 km (Table 2). The difference in the radius of maximum velocity is roughly proportional to the ratio of the Coriolis parameter at each ring's typical formation latitude. The overall ring diameters are considerably different with the maximum size of a Somali ring constrained by the width of the GOA. Although existing in situ observations are insufficient to determine the peak azimuthal velocities in Somali rings, estimates based on satellite altimetry suggest they are somewhat less intense than NBC rings even though flow through the Socotra Passage has been observed [e.g., *Schott et al.*, 1997] to be considerably stronger than that in the NBC upstream of the ring generation region [*Johns et al.*, 1998].

[34] Unlike NBC rings which are thought to play an important role in the intergyre transport of mass and heat in the Atlantic [e.g., *Johns et al.*, 2003] the Somali rings travel westward more slowly and are effectively trapped within the nearly closed GOA. In fact, one of the more interesting dynamical questions raised by these observations concerns the mechanism by which a ring may translate into an essentially closed basin of width comparable to the ring's diameter. While previous analytic theories of mid-ocean eddy self-propagation [e.g., *Nof*, 1983; *Cushman-Roisin et al.*, 1990] have been extended to deal with the contribution of sloping topography [e.g., *Jacob et al.*, 2002] we are not aware of any addressing a

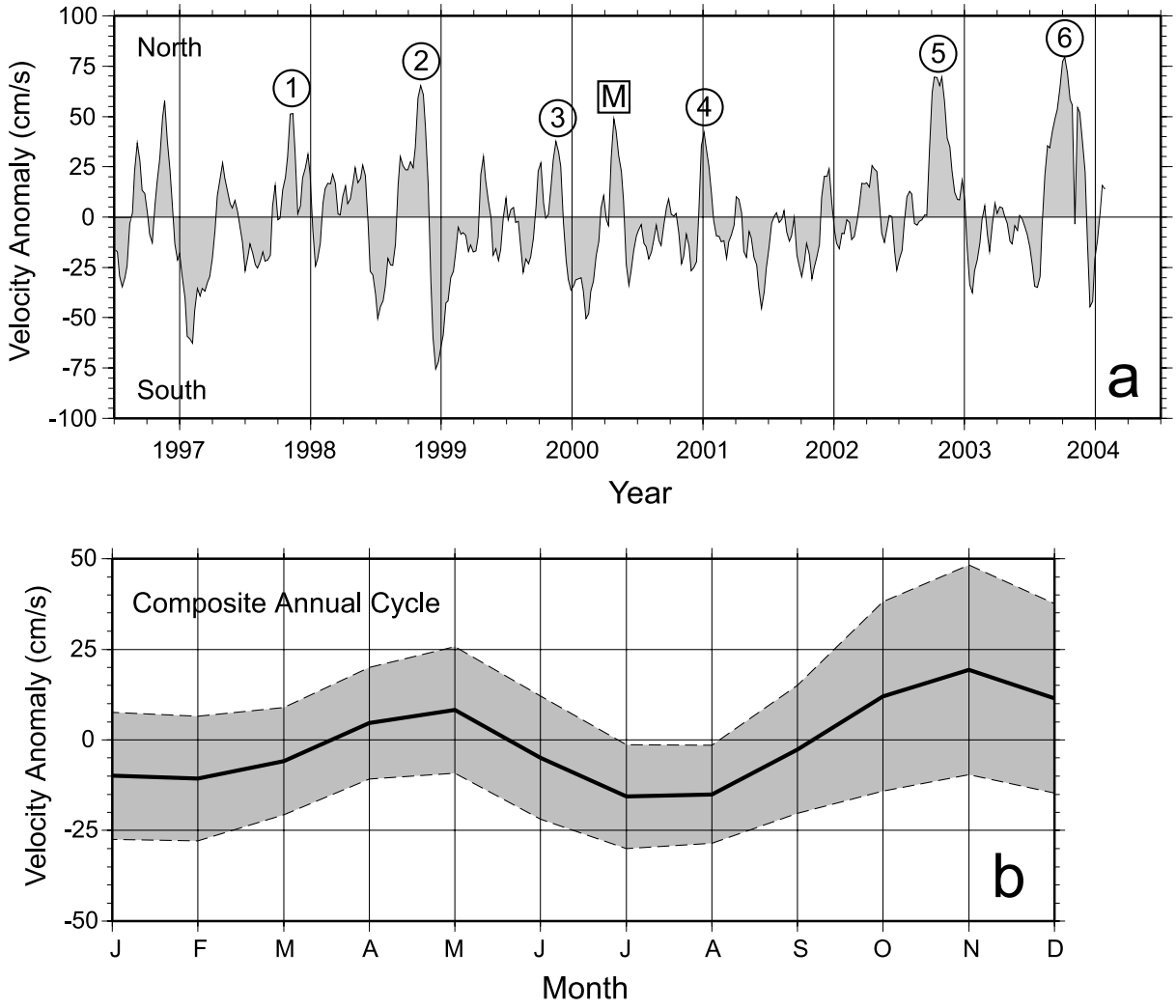

Figure 16. Application of an empirical model for velocity variability in the Socotra Passage based on satellite-derived sea surface slope variability. (a) Velocity anomaly in Socotra Passage as a function of time from mid-1996 through early 2004. Significant velocity peaks are coincident with ring generation events noted in Table 1. Note the dominant annual peak in November is often accompanied by a lesser peak in May; (b) Composite annual cycle generated by averaging the same data in monthly bins. The shaded region encompasses one standard deviation about the mean.

situation as complex as the GOA (i.e., sloping topography on both sides of a narrow zonal closed channel).

[35] On the basis of our analysis of satellite imagery there appear to be more vortices in the GOA than can be explained by the twice yearly ring generation mechanism described herein. For example, we observed an anticyclonic eddy in approximately the same location near 48°W in the central GOA during each of six successive Septembers (see Figure 12 for an example of one such feature). It is unclear whether these features were generated by an unresolved Socotra Passage jet, were generated locally within the GOA by some other mechanism, or translated into the GOA from elsewhere. Satellite observations (e.g., Figure 1) and some numerical model simulations (J. Kindle, personal communication, 2004) show mesoscale vortices moving toward the GOA both southwestward along the western boundary and westward directly from the interior Arabian Sea. Similar eddy-like mesoscale features are observed in all oceans

Table 2. Comparison of Somali Current and North Brazil Current Rings[a]

	North Brazil Current Rings	Somali Current Rings
Formation latitude	8°	12°
Radius of maximum velocity	125 km	75–100 km
Overall diameter	450 km	250 km
Azimuthal velocity	near 100 cm/s	at least 30–50 cm/s
Translation speed	12–17 cm/s	5–8 cm/s
Maximum observed life	5 months	5 months
Rings formed per year	8–9	1–2

[a]Characteristics of rings generated by the Somali Current north of the Socotra Passage compared with North Brazil Current (NBC) rings in the western tropical Atlantic. NBC values are after *Fratantoni and Glickson* [2002], *Johns et al.* [2003], and *Fratantoni and Richardson* [2006].

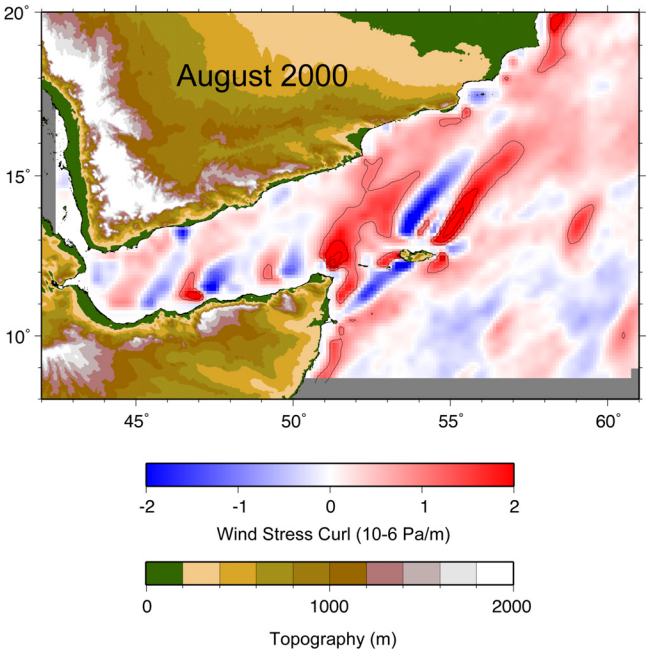

Figure 17. QuikSCAT wind stress curl averaged over the month of August 2000 during the height of the southwest monsoon. Note the strong relationship between dipole structures in the curl field and significant topographic features. The most intense curl pattern is evident downwind of the island of Socotra. Within the Gulf of Aden additional dipole structures are aligned with gaps between mountains along the northern coast of Somalia.

[e.g., *Wunsch*, 1981] and may have significant impact on local biological production [e.g., *McGillicuddy et al.*, 1998] (see Figure 1) but are generally impossible to trace backward in time to a discrete source.

[36] A possible additional source of mesoscale variability within the GOA itself involves eddy spin-up beneath localized wind stress curl maxima resulting from flow through gaps in the coastal mountain range of Somalia. Oceanographic impacts of wind jets in other locations, principally the eastern tropical Pacific, have been described by several authors [e.g., *Clarke*, 1988; *McCreary et al.*, 1989; *Chelton et al.*, 2004]. For example, a relationship has been demonstrated between wind jets passing through mountain gaps along the Pacific coast of Central America and the development of cold, nutrient-rich plumes which result in enhanced biological productivity. In the central Pacific, *Chavanne et al.* [2002] describe a mechanism of wind-forced eddy spin-up downwind of the Hawaiian islands. We find evidence in our data set that orographic forcing (i.e., wind enhanced and constrained by topography) could be responsible for the generation of some mid-GOA eddies, particularly during August when the southwest monsoon winds are most intense. Figure 17 illustrates wind stress curl computed from satellite scatterometer wind velocity fields [see *Chelton et al.*, 2004]. Note the relationship between curl patterns (and particularly the dipole structures) and gaps in the mountain range along the northern coast of Somalia. These curl anomalies are mainly confined to the southern half of the GOA (in the lee of the coastal mountains) as are most of the eddies observed in September (e.g., Figure 12).

[37] Several groups are presently investigating the region north of mountainous Socotra (P. Flament, personal communication, 2004) where a strong stress curl dipole is formed during the southwest monsoon. In addition to possible eddy spin-up within the GOA itself, an eddy formed in this position could translate westward into the gulf over a timescale consistent with our other observations. Complicating the interpretation of these curl measurements is the relationship between scatterometer-measured stress and unknown sea surface velocities. *Kelly et al.* [2001] reported that strong ocean surface velocities can significantly influence the stress measured by a satellite-based scatterometer such as QuikSCAT. It is therefore possible that the pattern of positive and negative wind stress curl in Figure 17 is a result, rather than a cause, of the string of eddies of alternating sign observed to populate the GOA. Significant additional investigation involving both satellite observations and numerical models will be required to fully resolve this issue.

6. Summary and Conclusions

[38] Analysis of 1997–2004 ocean color imagery and satellite altimetry indicates the periodic generation of westward translating anticyclonic rings from a retroflecting jet north of the Socotra Passage. We utilized a combination of satellite-based and in situ measurements to describe the formation and structure of these rings and explored the relationship between the episodically varying Socotra Passage transport and ring generation. The main findings of this study can be summarized as follows.

[39] 1. Immediately following the transition between the southwest (boreal summer) and northeast monsoons, a translating anticyclonic ring is generated by a portion of the Somali Current which accelerates northward through the Socotra Passage and retroflects near the mouth of the Gulf of Aden. There is considerable circumstantial evidence that ring generation also occurs in May following the opposite monsoon transition.

[40] 2. Cyclonic recirculation eddies form on the eastern flank of anticyclonic rings. Pairs of counterrotating vortices are observed to translate westward together and contribute to a pattern of alternating sign vortices observed to populate the GOA.

[41] 3. The anticyclonic rings are approximately 250 km in overall diameter with a radius of maximum (geostrophic) velocity of 75–100 km. Maximum altimeter-derived azimuthal velocities exceed 50 cm/s. The westward translation speed of both rings and cyclonic recirculation eddies is approximately 5–8 cm/s. Vortices of both sign are deep reaching and interact strongly with each other.

[42] 4. Ring formation is related to extreme northward transport events through the Socotra Passage. Historical moored current meter records and a simple model of transport variability based on satellite-based sea level measurements indicate that that such extremes follow both the October and April monsoon transitions.

[43] 5. Additional eddies translate into the region from the Arabian Sea and interior Indian Ocean and still others may be formed locally within the GOA. We find evidence that

wind jets associated with mountainous topography on the northern coast of Somalia could be responsible for the generation of mid-GOA eddies, particularly during August when the southwest monsoon winds are most intense.

[44] In this article we have presented new observations of previously undocumented phenomena in a fairly remote area of the world ocean. It is our hope that these observations inspire further observational, numerical, and theoretical studies. Synthesis of these measurements with numerical ocean models should be particularly instructive and are needed in order to address outstanding questions regarding the generation, structure, translation, and evolution of these interesting mesoscale features. For example, why does Socotra Passage flow intensify following the monsoon transitions? How is Socotra Passage transport related to the seasonally modulated Great Whirl and Socotra Gyre? How does a vortex in contact with both sidewalls propagate westward into a closed channel? Can localized wind stress curl spin up persistent eddies? A validated numerical model will provide the most efficient framework in which to address such questions. Initial comparisons of remote and in situ observations with a high-resolution assimilating numerical model (the Naval Research Laboratory (NRL) Global Layered Ocean Model; [see *Smedstad et al.*, 2003]) suggests that the episodic Socotra Passage jet and ring-shedding are reasonably approximated (J. Kindle, personal communication, 2004). Substantial additional investigation, including new in situ measurements, are required to correctly interpret the wide spectrum of eddy variability present in the numerical model and relate it to discrete observations.

[45] **Acknowledgments.** This investigation is a component of the Red Sea Outflow Experiment (REDSOX) sponsored by the U.S. National Science Foundation through grants OCE 98-18464 and OCE 04-24647 to the Woods Hole Oceanographic Institution and OCE 98-19506 and OCE 03-51116 to the University of Miami. We thank Fritz Schott for permission to use the Socotra Passage current meter records and Rainer Zantopp for facilitating access to these data. Deb Glickson was instrumental in the initial preparation and analysis of the SeaWiFS imagery. The ocean color data used herein were provided by the SeaWiFS Project at Goddard Space Flight Center. The data were obtained from the Goddard Distributed Active Archive Center under the auspices of NASA. Use of these data is in accord with the SeaWiFS Research Data Use Terms and Conditions Agreement. The altimeter products were produced as part of the Environment and Climate EU Enact project (EVK2-CT2001-00117) and distributed by AVISO with support from CNES. Quikscat wind data were obtained from the NASA Physical Oceanography Distributed Active Archive Center (PO.DAAC) at the Jet Propulsion Laboratory, Pasadena, California. Pierre Flament and Cedric Chavanne introduced us to the idea of local wind stress curl forcing as a potential eddy generation mechanism. We thank them for their assistance with an initial subset of the Quikscat data. We thank John Kindle for providing output from various NRL model simulations. Heather Furey processed the RAFOS float data. Mike Caruso reviewed an early version of this manuscript and provided valuable suggestions. Discussions with Claudia Cenedese were particularly helpful.

References

Anderson, D. L. T., and P. B. Rowlands (1976), The Somali Current response to the Southwest Monsoon: The relative importance of local and remote forcing, *J. Mar. Res.*, *34*, 395–417.

Beal, L. M., A. Field, and A. L. Gordon (2000), Spreading of Red Sea overflow waters in the Indian Ocean, *J. Geophys. Res.*, *105*, 8537–8548.

Bower, A. S., D. M. Fratantoni, W. E. Johns, and H. Peters (2002), Gulf of Aden eddies and their impact on Red Sea Water, *Geophys. Res. Lett.*, *29*(21), 2025, doi:10.1029/2002GL015342.

Bower, A. S., W. E. Johns, D. M. Fratantoni, and H. Peters (2005), Equilibration and circulation of Red Sea Outflow Water in the western Gulf of Aden, *J. Phys. Oceanogr.*, *35*, 1963–1985.

Brandt, P., M. Dengler, A. Rubino, D. Quadfasel, and F. Schott (2003), Intraseasonal variability in the southwestern Arabian Sea and its relation to the seasonal circulation, *Deep Sea Res., Part II*, *12–13*, 2129–2141.

Broecker, W. S., and T. H. Peng (1982), *Tracers in the Sea*, 690 pp., Lamont-Doherty Earth Observatory, Palisades, N. Y.

Brown, O. B., J. G. Bruce, and R. H. Evans (1980), Evolution of sea surface temperature in the Somali Basin during the southwest monsoon of 1979, *Science*, *209*, 595–597.

Brown, O. B., D. B. Olson, J. W. Brown, and R. H. Evans (1983), Satellite infrared observation of the kinematics of a warm-core ring, *Aust. J. Mar. Freshwater Res.*, *34*, 535–545.

Bruce, J. G. (1979), Eddies off the Somali coast during the southwest monsoon, *J. Geophys. Res.*, *84*, 7742–7748.

Bruce, J. G., and W. H. Beatty (1985), Some observations of the coalescing of Somali eddies and a description of the Socotra eddy, *Oceanol. Acta*, *8*, 207–219.

Cenedese, C., and J. A. Whitehead (2000), Eddy shedding from a boundary current around a cape over a sloping bottom, *J. Phys. Oceanogr.*, *30*, 1514–1531.

Chavanne, C., P. Flament, R. Lumpkin, B. Dousset, and A. Bentamy (2002), Scatterometer observations of wind variations induced by oceanic islands: Implications for wind-driven ocean circulation, *Can. J. Remote Sens.*, *28*, 466–474.

Chelton, D. B., M. G. Schlax, M. H. Freilich, and R. F. Milliff (2004), Satellite measurements reveal persistent small-scale features in ocean winds, *Science*, *303*, 978–983.

Clarke, A. J. (1988), Inertial wind path and sea surface temperature patterns near the Gulf of Tehuantepec and Gulf of Papagayo, *J. Geophys. Res.*, *93*, 15,491–15,501.

Cushman-Roisin, B., E. P. Chassignet, and B. Tang (1990), Westward motion of mesoscale eddies, *J. Phys. Oceanogr.*, *20*, 758–768.

Defant, A. (1961), *Physical Oceanography*, vol. 1, 729 pp., Elsevier, New York.

Didden, N., and F. Schott (1993), Eddies in the North Brazil Current retroflection region observed by Geosat altimetry, *J. Geophys. Res.*, *98*, 20,121–20,131.

Ducet, N., P.-Y. Le Traon, and G. Reverdin (2000), Global high resolution mapping of ocean circulation from TOPEX/Poseidon and ERS-1 and -2, *J. Geophys. Res.*, *105*, 19,477–19,498.

Düing, W. (1970), *The Monsoon Regime of the Currents in the Indian Ocean*, 68 pp., East-West Cent. Press, Univ. of Hawaii, Honolulu.

Düing, W., R. L. Molinari, and J. C. Swallow (1980), Somali Current: Evolution of surface flow, *Science*, *209*, 588–589.

Evans, R. H., and O. B. Brown (1981), Propagation of thermal fronts in the Somali Current system, *Deep Sea Res., Part A*, *28*, 521–527.

Findlay, A. G. (1866), *A Directory for the Navigation of the Indian Ocean*, 1062 pp., Richard Holmes Laurie, London.

Fischer, J., F. Schott, and L. Stramma (1996), Currents and transports of the Great Whirl-Socotra Gyre system during the summer monsoon, August 1993, *J. Geophys. Res.*, *101*, 3573–3587.

Fratantoni, D. M., and D. A. Glickson (2002), North Brazil Current ring generation and revolution observed with SeaWiFS, *J. Phys. Oceanogr.*, *32*, 1058–1074.

Fratantoni, D. M., and P. L. Richardson (2006), The evolution and demise of North Brazil Current Rings, *J. Phys. Oceanogr.*, *36*(7), 1241–1264.

Furey, H. H., A. S. Bower, and D. M. Fratantoni (2005), Red Sea Outflow Experiment (REDSOX) DLD2 RAFOS float data report February 2001–March 2003, *Woods Hole Oceanogr. Inst. Tech. Rep. WHOI-2005–01*, Woods Hole, Mass.

Gordon, A. L., J. R. E. Lutjeharms, and M. L. Grundlingh (1987), Stratification and circulation at the Agulhas Retroflection, *Deep Sea Res., Part A*, *34*, 565–599.

Hooker, S. B., W. E. Esaias, G. C. Feldman, W. W. Gregg, and C. R. McClain (1992), An overview of SeaWiFS and ocean color, *NASA Tech. Memo., 104566*.

Jacob, J. P., E. P. Chassignet, and W. K. Dewar (2002), Influence of topography on the propagation of isolated eddies, *J. Phys. Oceanogr.*, *32*, 2848–2869.

Johns, W. E., T. N. Lee, F. A. Schott, R. J. Zantopp, and R. H. Evans (1990), The North Brazil Current retroflection: Seasonal structure and eddy variability, *J. Geophys. Res.*, *95*, 22,103–22,120.

Johns, W. E., T. N. Lee, R. C. Beardsley, J. Candela, R. Limeburner, and B. Castro (1998), Annual cycle and variability of the North Brazil Current, *J. Phys. Oceanogr.*, *28*, 103–128.

Johns, W., H. Peters, R. Zantopp, A. Bower, and D. Fratantoni (2001), CTD/O2 measurements collected aboard the R/V Knorr, February–March 2001; REDSOX-1, *Tech. Rep. 2001–01*, 10 pp., plus append., Univ. of Miami, Miami, Fla.

Johns, W. E., R. J. Zantopp, and G. J. Goni (2003), Cross-gyre transport by North Brazil Current Rings, in *Interhemispheric Water Exchange in the*

Atlantic Ocean, edited by G. J. Goni and P. Malanotte-Rizzoli, *Elsevier Oceanogr. Ser.*, *68*, 411–441.

Kalnay, E., et al. (1996), The NCEP/NCAR 40-year re-analysis project, *Bull. Am. Meteorol. Soc.*, *77*, 437–471.

Kelly, K. A., S. Dickinson, M. J. McPhaden, and G. C. Johnson (2001), Ocean currents evident in the satellite wind data, *Geophys. Res. Lett.*, *28*, 2469–2472.

Le Traon, P.-Y., and G. Dibarboure (1999), Mesoscale mapping capabilities of multi-satellite altimeter missions, *J. Atmos. Oceanic Technol.*, *16*, 1208–1223.

Lukas, R., E. Firing, P. Hacker, P. L. Richardson, C. A. Collins, R. Fine, and R. Gammon (1991), Observations of the Mindanao Current during the western equatorial Pacific Ocean circulation study, *J. Geophys. Res.*, *96*, 7089–7104.

Matsumoto, Y., T. Kagimoto, M. Yoshida, M. Fukada, N. Hirose, and T. Yamagata (2001), Intraseasonal eddies in the Sulawesi Sea simulated in an ocean general circulation model, *Geophys. Res. Lett.*, *28*, 1631–1634.

McClain, C. R., M. L. Cleave, G. C. Feldman, W. W. Gregg, S. B. Hooker, and N. Kuring (1998), Science quality SeaWiFS data for global biosphere research, *Sea Technol.*, September, 10–16.

McCreary, J. P., H. S. Lee, and D. B. Enfield (1989), The response of the coastal ocean to strong offshore winds: With application to circulation in the Gulf of Tehuantepec and Papagayo, *J. Mar. Res.*, *47*, 81–109.

McGillicuddy, D. J., A. R. Robinson, D. A. Siegel, H. W. Jannasch, R. Johnson, T. D. Dickey, J. McNeil, A. F. Michaels, and A. H. Knap (1998), Influence of mesoscale eddies on new production in the Sargasso Sea, *Nature*, *394*, 263–265.

Molinari, R. L., D. Olson, and G. Reverdin (1990), Surface current distributions in the tropical Indian Ocean derived from compilations of surface buoy trajectories, *J. Geophys. Res.*, *95*, 7217–7238.

Nof, D. (1983), On the migration of isolated eddies with application to Gulf Stream rings, *J. Mar. Res.*, *41*, 399–425.

Nof, D. (1996), Why are rings regularly shed in the western equatorial Atlantic but not in the western Pacific?, *Prog. Oceanogr.*, *38*, 417–451.

Olson, D. B. (1991), Rings in the ocean, *Annu. Rev. Earth Planet. Sci.*, *19*, 283–311.

Olson, D. B., G. L. Hitchcock, R. A. Fine, and B. A. Warren (1993), Maintenance of the low-oxygen layer in the central Arabian Sea, *Deep Sea Res., Part I*, *40*, 673–685.

Peters, H., and W. E. Johns (2006), Bottom layer turbulence in the Red Sea outflow plume, *J. Phys. Oceanogr.*, in press.

Prasad, T. G., and M. Ikeda (2001), Spring evolution of Arabian Sea High in the Indian Ocean, *J. Geophys. Res.*, *106*, 31,085–31,098.

Prasad, T. G., M. Ikeda, and J. L. McClean (2005), Structure and mechanisms of the Arabian Sea variability during the winter monsoon, *Deep Sea Res., Part I*, *52*, 1155–1177.

Qiu, B., M. Mao, and Y. Kashino (1999), Intraseasonal variability in the Indo-Pacific throughflow and the regions surrounding the Indonesian Seas, *J. Phys. Oceanogr.*, *29*, 1599–1618.

Schott, F. (1983), Monsoon response of the Somali Current and associated upwelling, *Prog. Oceanogr.*, *12*, 357–381.

Schott, F. A., and J. Fischer (2000), Winter monsoon circulation of the northern Arabian Sea and Somali Current, *J. Geophys. Res.*, *105*, 6359–6376.

Schott, F., and D. R. Quadfasel (1982), Variability of the Somali Current system during the onset of the southwest monsoon, 1979, *J. Phys. Oceanogr.*, *12*, 1343–1357.

Schott, F., J. Fischer, U. Garternicht, and D. Quadfasel (1997), Summer monsoon response of the northern Somali Current, 1995, *Geophys. Res. Lett.*, *24*, 2565–2568.

Shewchuck, J. R. (1996), Triangle: Engineering a 2D quality mesh generator and delaunay triangulator, paper presented at First Workshop on Applied Computational Geometry, Assoc. for Comput. Mach., Philadelphia, Pa.

Simmons, R. C., M. E. Luther, J. J. O'Brien, and D. M. Legler (1988), Verification of a numerical ocean model of the Arabian Sea, *J. Geophys. Res.*, *93*, 15,437–15,453.

Smedstad, O. M., H. E. Hurlburt, E. J. Metzger, R. C. Rhodes, J. F. Shriver, A. J. Wallcraft, and A. B. Kara (2003), An operational eddy resolving 1/16° Global Ocean Nowcast/Forecast System, *J. Mar. Syst.*, *40–41*, 341–361.

Swallow, J. C., and J. G. Bruce (1966), Current measurements off the Somali coast during the southwest monsoon of 1964, *Deep Sea Res.*, *13*, 861–888.

Visbeck, M., and F. Schott (1992), Analysis of seasonal current variations in the western equatorial Indian Ocean: Direct measurements and GFDL model comparison, *J. Phys. Oceanogr.*, *22*, 1112–1128.

Wunsch, C. (1981), Low-frequency variability of the sea, in *Evolution of Physical Oceanography*, editedy by B. A. Warren and C. Wunsch, pp. 342–375, MIT Press, Cambridge, Mass.

A. S. Bower and D. M. Fratantoni, Department of Physical Oceanography, Woods Hole Oceanographic Institution, Woods Hole, MA 02543, USA. (dfratantoni@whoi.edu)

W. E. Johns and H. Peters, Division of Meteorology and Physical Oceanography, Rosenstiel School of Marine and Atmospheric Science, University of Miami, Miami, FL 33149, USA.